

SEDIMENTOLOGYthe journal of the
International Association of Sedimentologists**Stratigraphy and sedimentary evolution of a modern macro-tidal incised valley – an analogue for reservoir facies and architecture**

Journal:	<i>Sedimentology</i>
Manuscript ID	SED-2020-OM-333.R2
Manuscript Type:	Original Manuscript
Date Submitted by the Author:	n/a
Complete List of Authors:	McGhee, Claire; Newcastle University, School of Natural and Environmental Sciences Worden, Richard; University of Liverpool School of Environmental Sciences Muhammed, Dahiru; University of Liverpool School of Environmental Sciences Simon, Naboth; University of Liverpool School of Environmental Sciences Acikalin, Sanem; Newcastle University, School of Natural and Environmental Sciences Griffiths, Joshua ; BP Exploration Co Ltd Wooldridge, Luke; BP Exploration Co Ltd Utley, James; University of Liverpool School of Environmental Sciences Verhagen, Iris; University of Liverpool, Earth Ocean and Ecological Sciences van der Land, Cees; Newcastle University, School of Natural and Environmental Sciences
Keywords:	Incised-valley, Ravenglass Estuary, Macro-tidal, Connectivity, Sandstone Reservoir Quality, Sequence Stratigraphy, Tide-dominated

SCHOLARONE™
Manuscripts

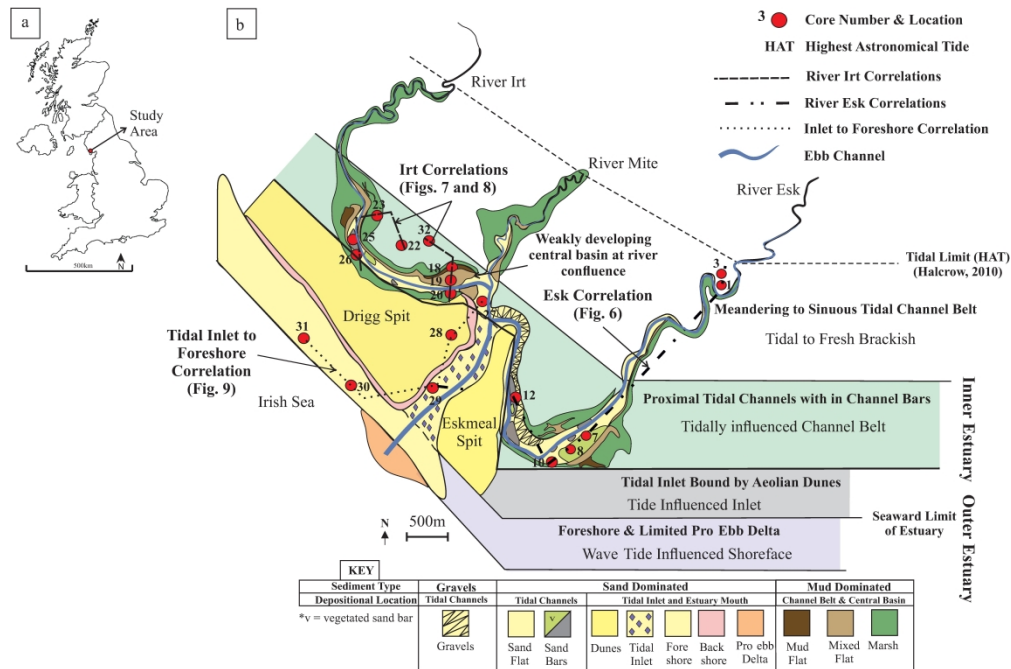


Figure 1. a) Location map indicating Ravenglass Estuary, Cumbria, UK with a red circle. b) Map of present-day estuarine zones and sub-depositional environments of Ravenglass Estuary. The estuary outer is defined by the landward limit of the tidal inlet. The outer estuary consists of a tidal inlet bound by the Drigg and Eskmeal Spits (darker yellow), foreshore (dark yellow) and a pro-ebb delta (orange). The inner estuary consists of proximal tidal channels (the rivers Irt, Esk and Mite) with a distal meandering tidal channel belt, proximal tidal sand bars (light green), mixed flats, mudflats and extensive salt marsh (dark green). The map also indicates the position of the 19 Holocene cores (red circles) used in the study. Correlation panels for the Holocene cores are shown by a single dashed line for the River Irt, dashed and dotted line for the River Esk and a dotted line for the tidal inlet to foreshore.

293x195mm (600 x 600 DPI)

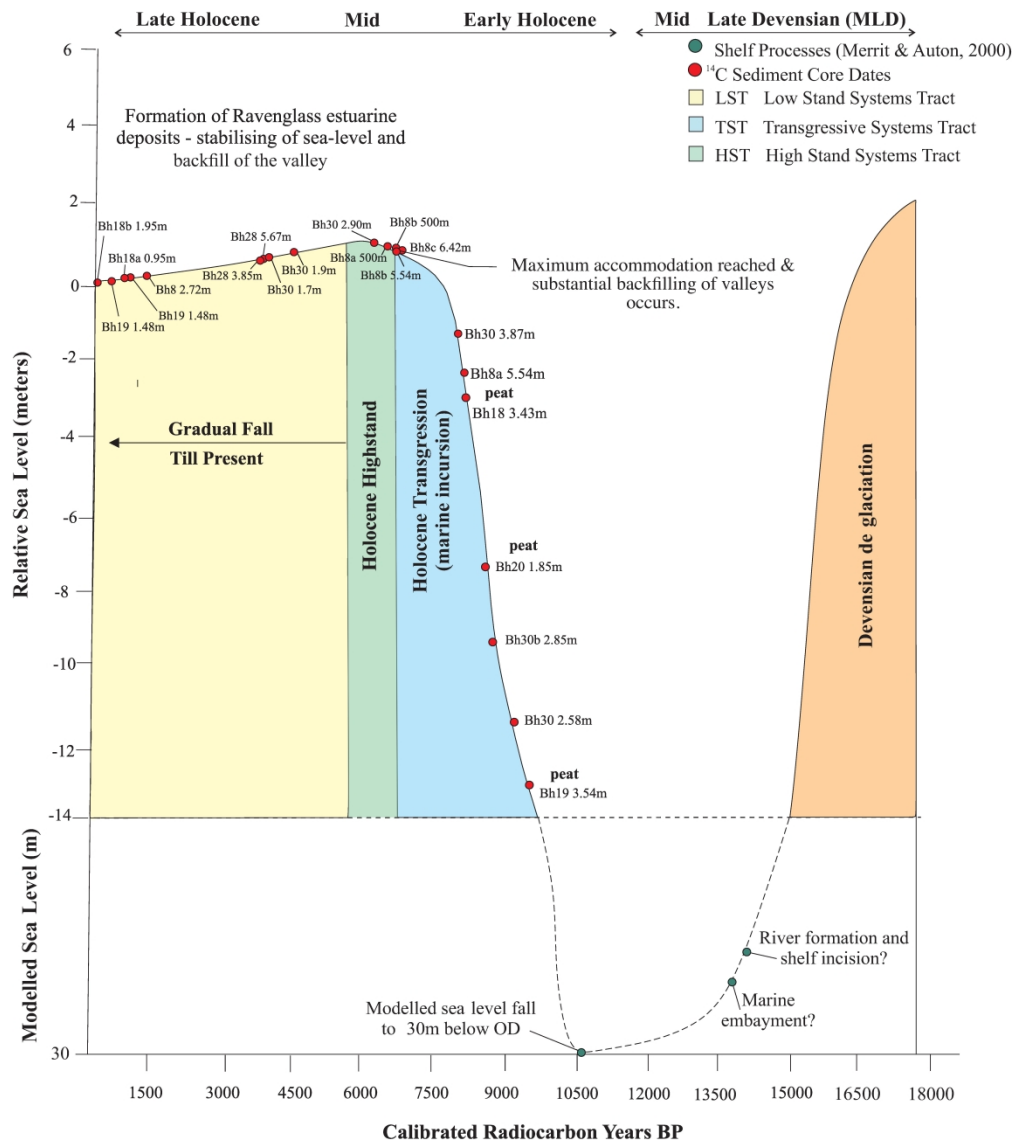


Figure 2. Lloyd et al., (2012) Devensian-Holocene sea-level curve with all new ¹⁴C dates and depths plotted from Ravenglass Estuary cores (red circles). The Devensian glacial lowstand, when isostatic rebound outstripped sea-level rise, between 12,000-10,500 yrs BP inducing enhanced fluvial incision in the lower valleys. This was followed by a rapid transgression, which was characterised by a phase of relative sea-level rise, occurring between c.10,500-6,000 BP. During this time, net sediment transport was landward. A minor fall in relative sea level from 5,000 yrs BP to the present day, resulting in dominant estuarine conditions (adapted from Lloyd et al., 2012).

267x301mm (600 x 600 DPI)

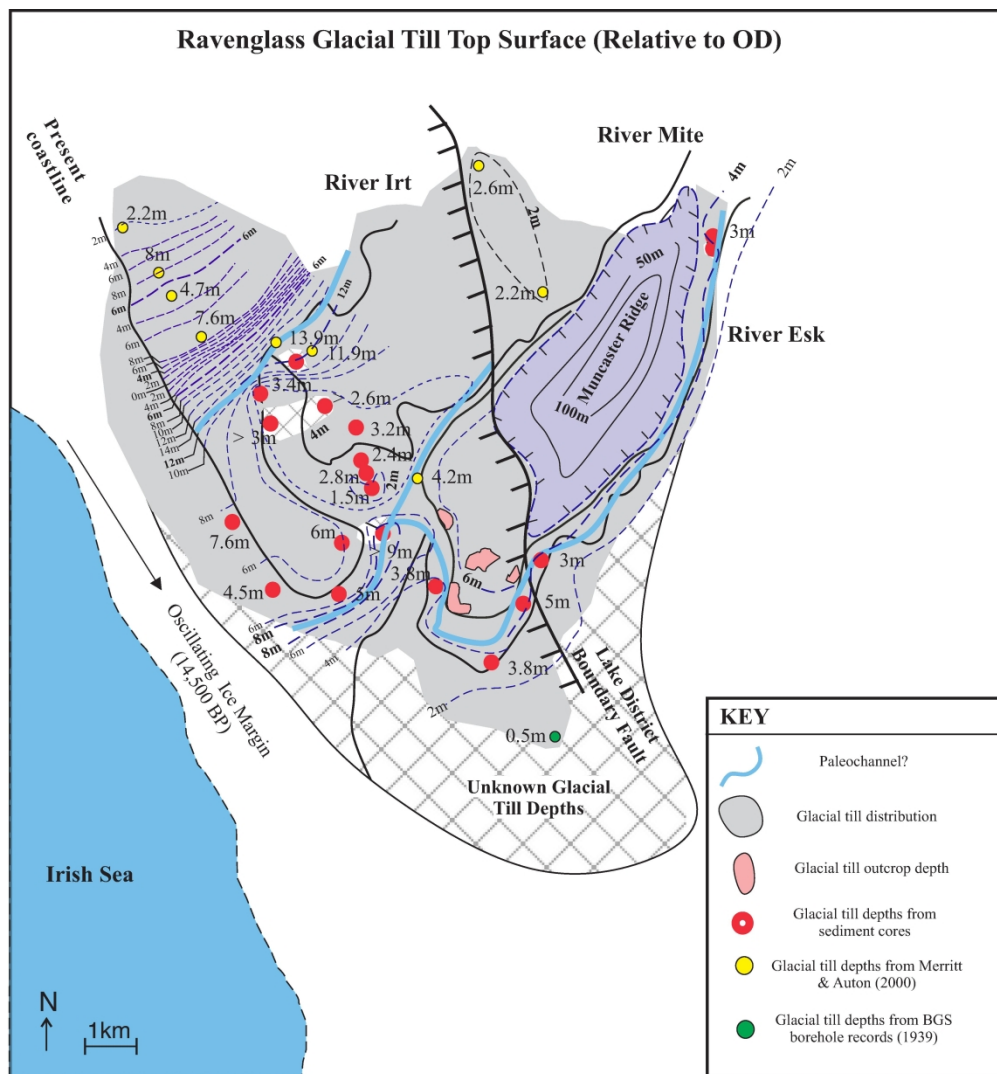


Figure 3. Contoured surface map of the Ravenglass Glacial Till Member (RGTM) based on outcrop data (pink), the drilled sediment cores (red circles), data from Merritt & Auton (2000) (yellow) and the British Geological Survey repository (green). The white squared box under the present-day Eskmeal Spit is unknown depths to the Ravenglass Glacial Till Member (RGTM). The blue lines indicate the palaeo-channels of the River Irt, Mite and Esk. Note the steep sided, deeper channel of the River Irt to the NW and the topographical high between the River Irt and River Mite. The river Esk flows around an Ordovician Granitic fell (purple) known as Muncaster Ridge, bound by the Lake District Boundary Fault.

183x196mm (600 x 600 DPI)

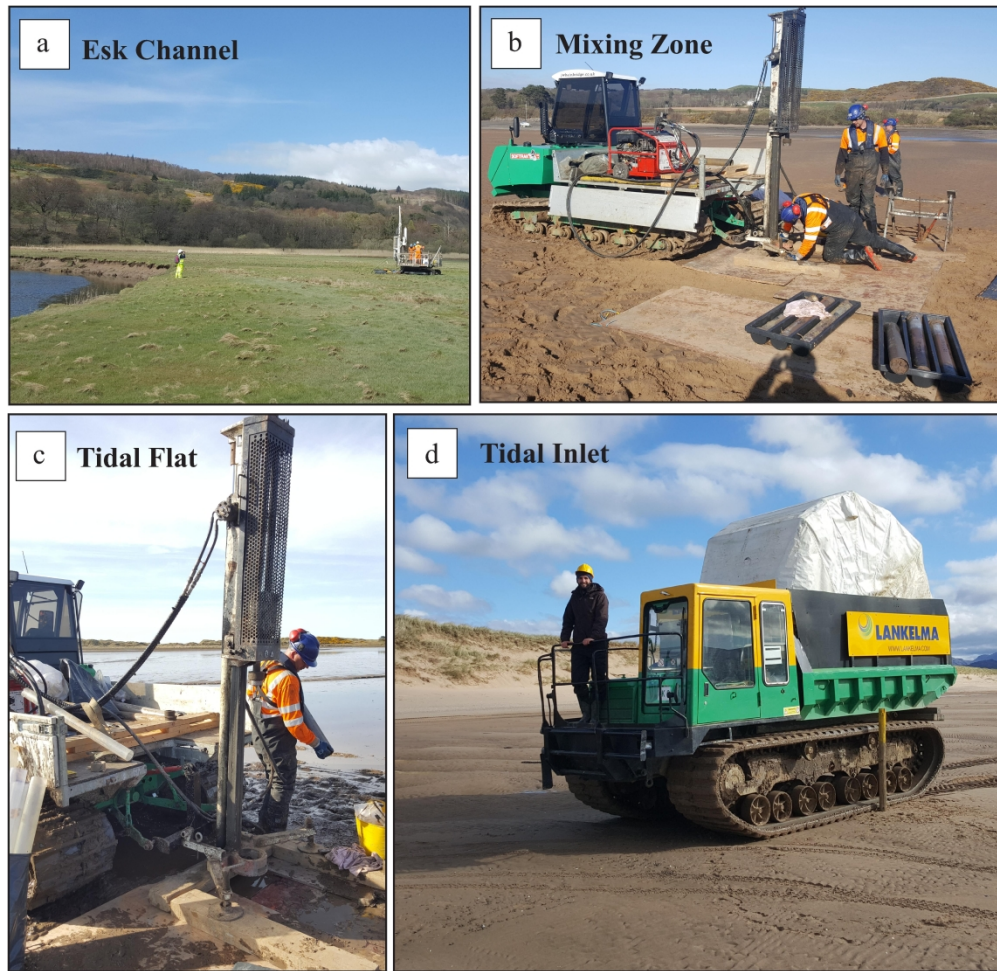


Figure 4. Drilling locations and rigs used to core the Ravenglass valley-fill. a) River Esk tidal channel with Pioneer b) mixing zone of the rivers c) tidal flat and d) tidal inlet.

195x189mm (600 x 600 DPI)

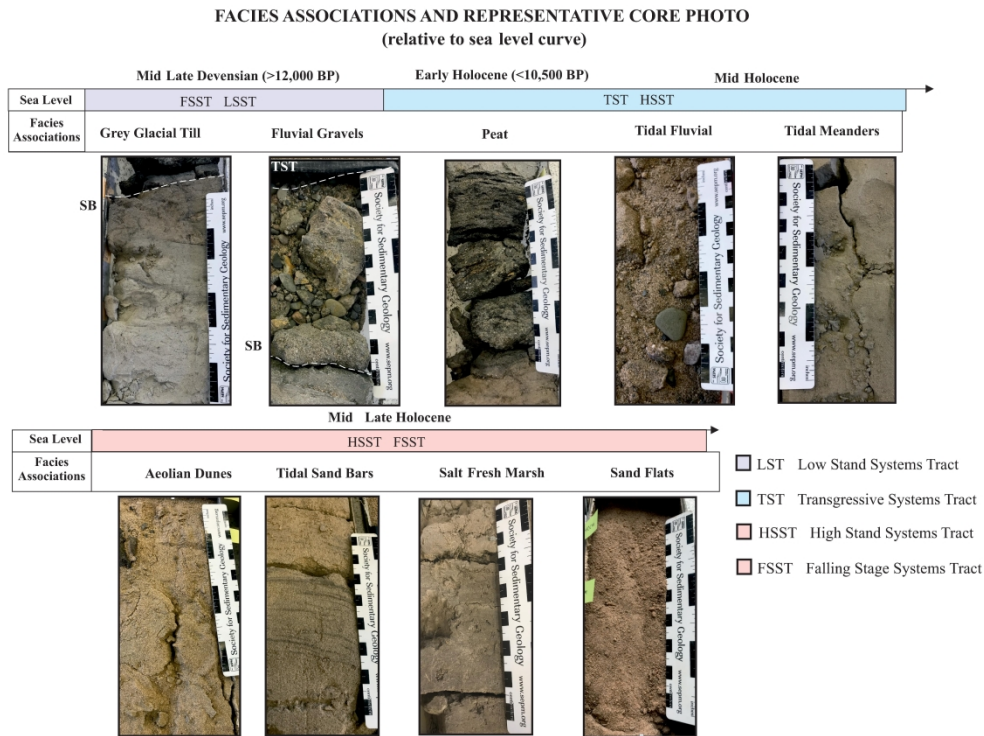


Figure 5. Facies and representative core photo of Ravenglass incised valley fill. From left to right (top to bottom): The Devensian Ravenglass Glacial Till Member (RGTM), a grey diamicton till that is a poorly sorted with a chaotic internal structure. The fluvial gravels composed of gravel grade material and coarse sand. The laminated black to brown coloured peats is composed of leafy organic material. The tidal fluvial sands composed of medium to coarse grained sand with pebbles and disarticulated shell fragments. The aeolian dunes composed of fine to medium grained cross-bedded sands. The tidal meanders are fine to medium grained, interbedded muds and sands that fine upwards. The tidal sand bars show an overall fining upwards profile from coarse-grained sands to interbedded muds and sand. Vegetated tidal sand bars are commonly capped with salt or fresh marsh. The marsh is composed of interbedded silt and mud which is often moderately bioturbated and roots are present near the top. The sand flats are fine grained with some disarticulated shell fragments.

275x202mm (600 x 600 DPI)

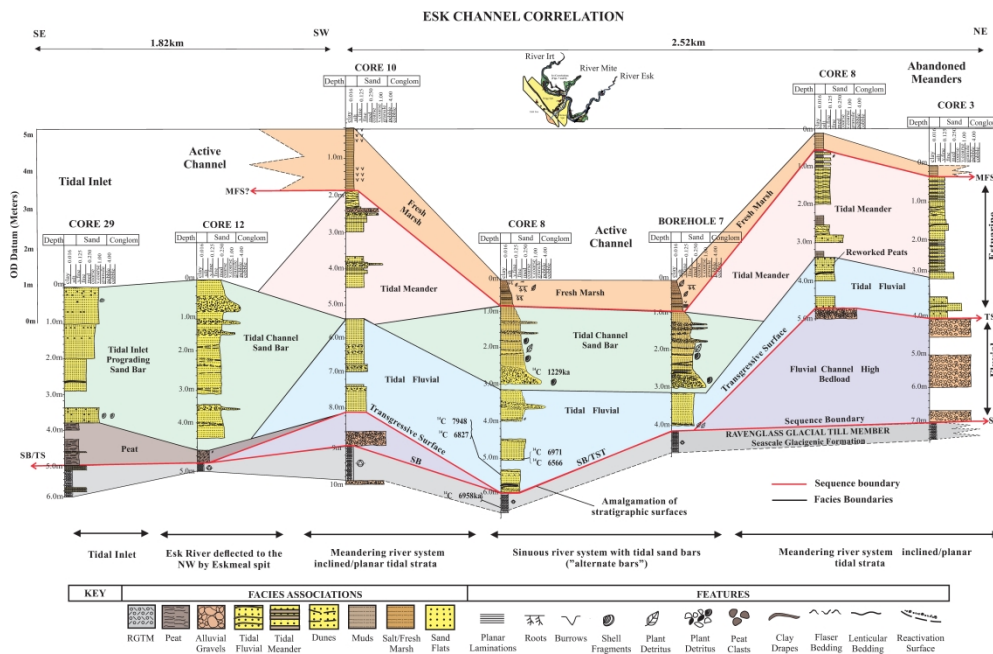


Figure 6. River Esk correlation panel from the Devensian to present-day highlighting inner estuarine facies and sequence stratigraphic boundaries marked by the dashed black lines. The red dashed lines highlight uncertainties in the correlation, especially associated with the tidal meander sediments. Also highlighted is the meandering-sinuous-meander nature of the sediment with channel tidal bars (alternate bars) and upstream point-bars, indicative of tide-dominated systems.

417x268mm (600 x 600 DPI)

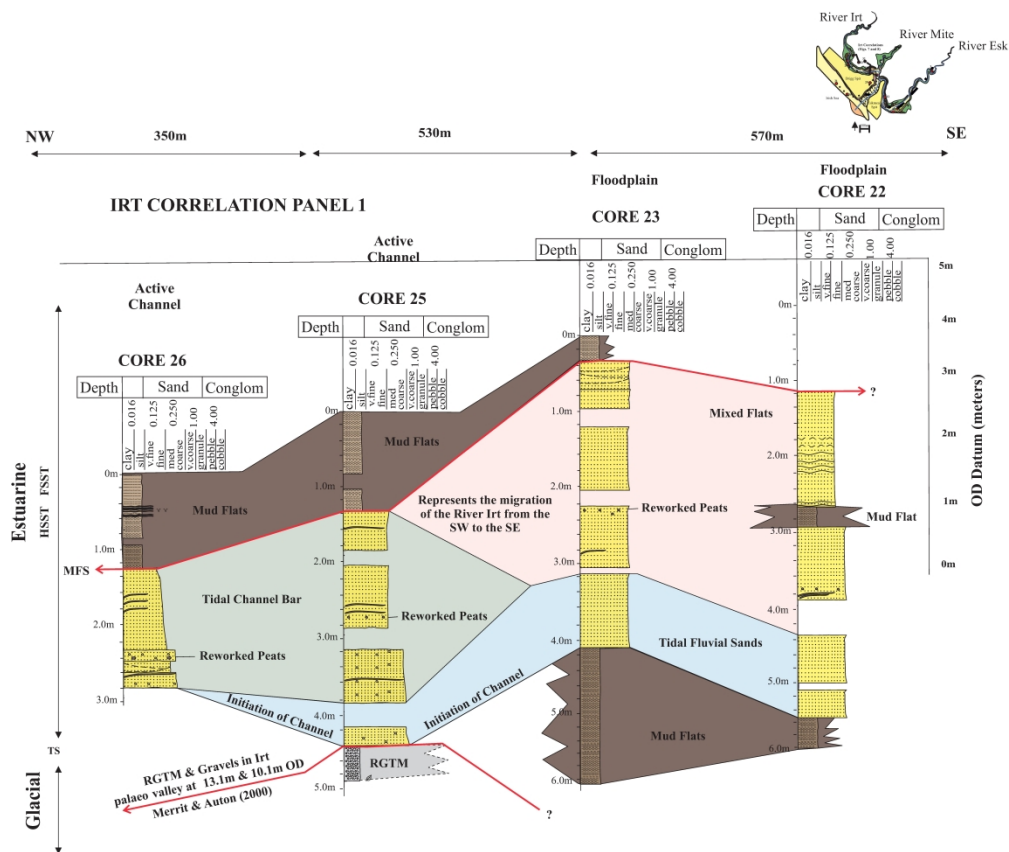


Figure 7. River Irt correlation panel 1. The River Irt panel shows the inner estuarine facies and sequence boundaries marked by the solid red lines. Note the lack of sequence boundaries with the exception of core 25 which has the RGTM. Above the RGTM are fluvial tidal bars between core 25 and 26, channel sands and mud flats in cores 22 and 23. The sequence boundary is located deeper in the Irt palaeo-channel at 13.1m (OD) indicated by the red arrow (Merritt & Auton, 2000).

338x285mm (600 x 600 DPI)

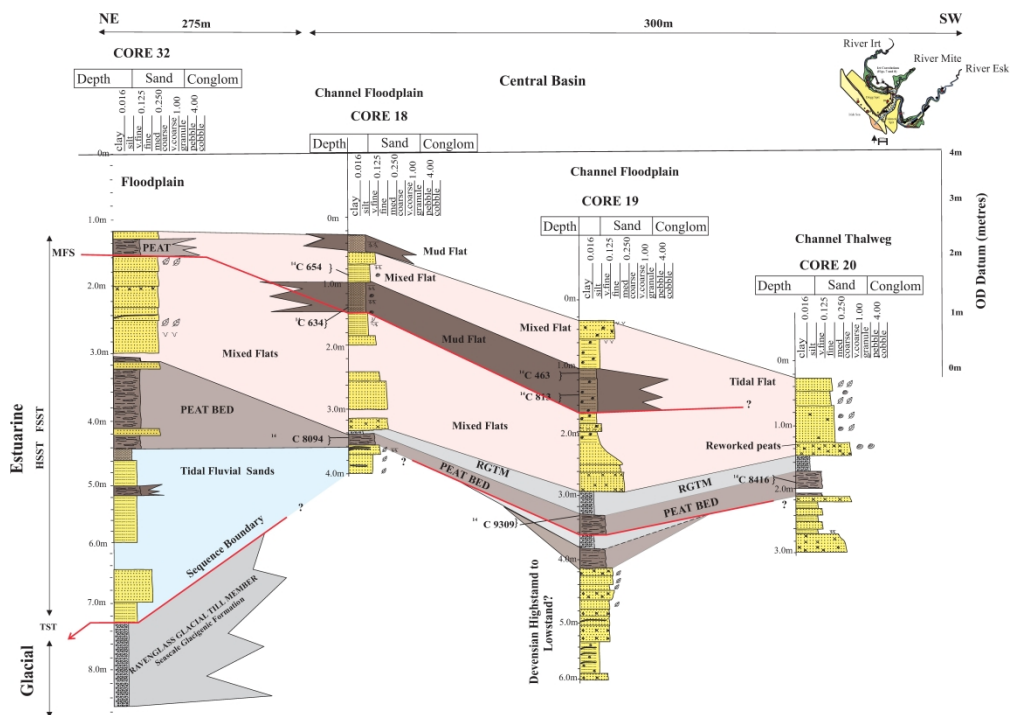


Figure 8. River Irt correlation 2. The panel indicates the River Irt and part of the central basin from the Devensian to present-day with sequence boundaries shown by a red solid line. The Ravenglass Glacial Till Member (RGTM) is partially correlatable between cores. The most abundant peat accumulations (14C 9,309, 8416 and 8094 BP) and fine-grained sediment occur here, implying it was a relatively sheltered area above the valley wall throughout most of the low-stand and Holocene transgression (also supported by the back of gravel beds above Ravenglass Glacial Till Member (RGTM)).

384x271mm (600 x 600 DPI)

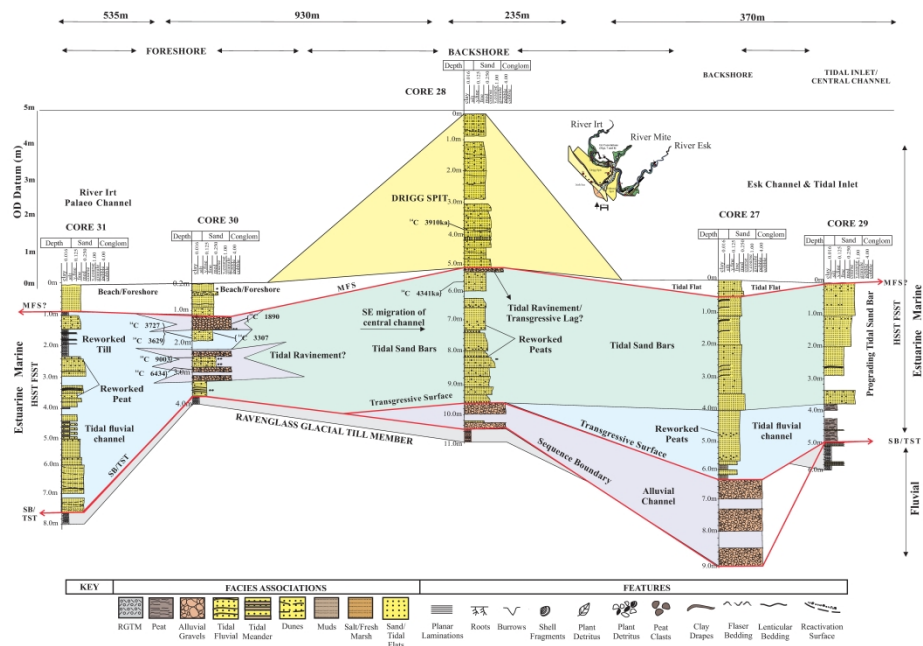
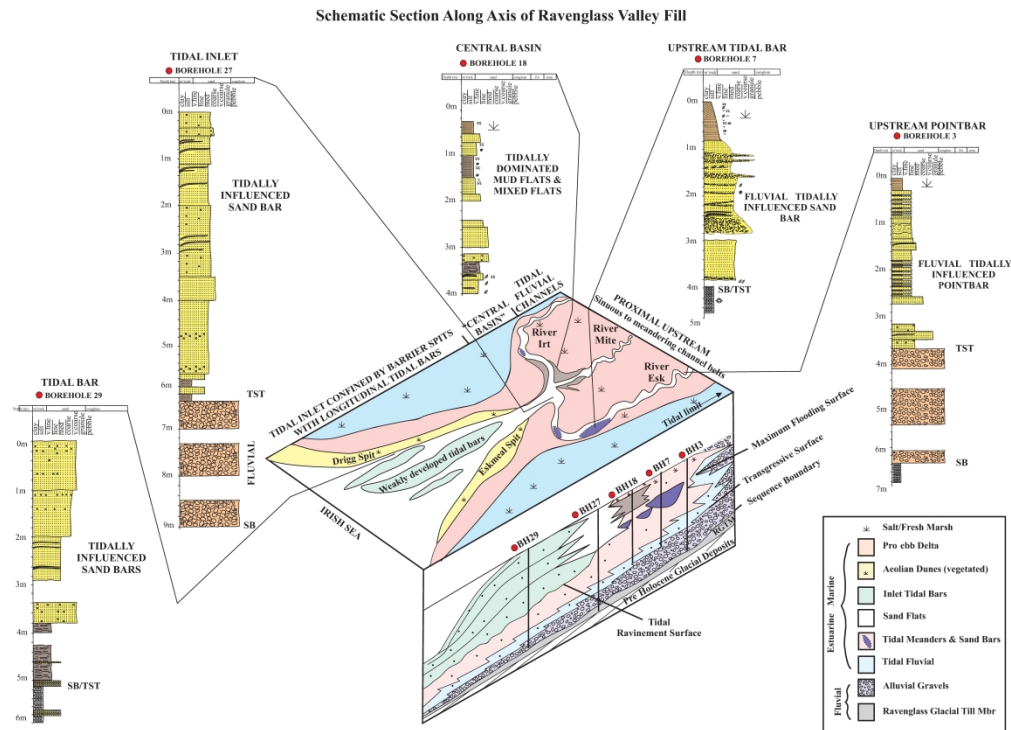


Figure 9. The foreshore and tidal inlet correlation panel highlighting the outer estuarine facies and sequence stratigraphic surfaces shown by the solid red line. The sequence boundary here becomes amalgamated with the transgressive surface near the valley high's shown by core 30 (potentially a point of tidal ravinement). Core 31 indicates the sequence boundary going deeper into the River Irt palaeo-channel also shown in the first River Irt correlation panel. Reworked peats are also limited to the Irt palaeo-channels. Cores 28 and 29 are in the tidal inlet and show the prograding sand bars. Core 28 shows the evolution of the Drigg Spit.

452x288mm (600 x 600 DPI)



398x288mm (600 x 600 DPI)

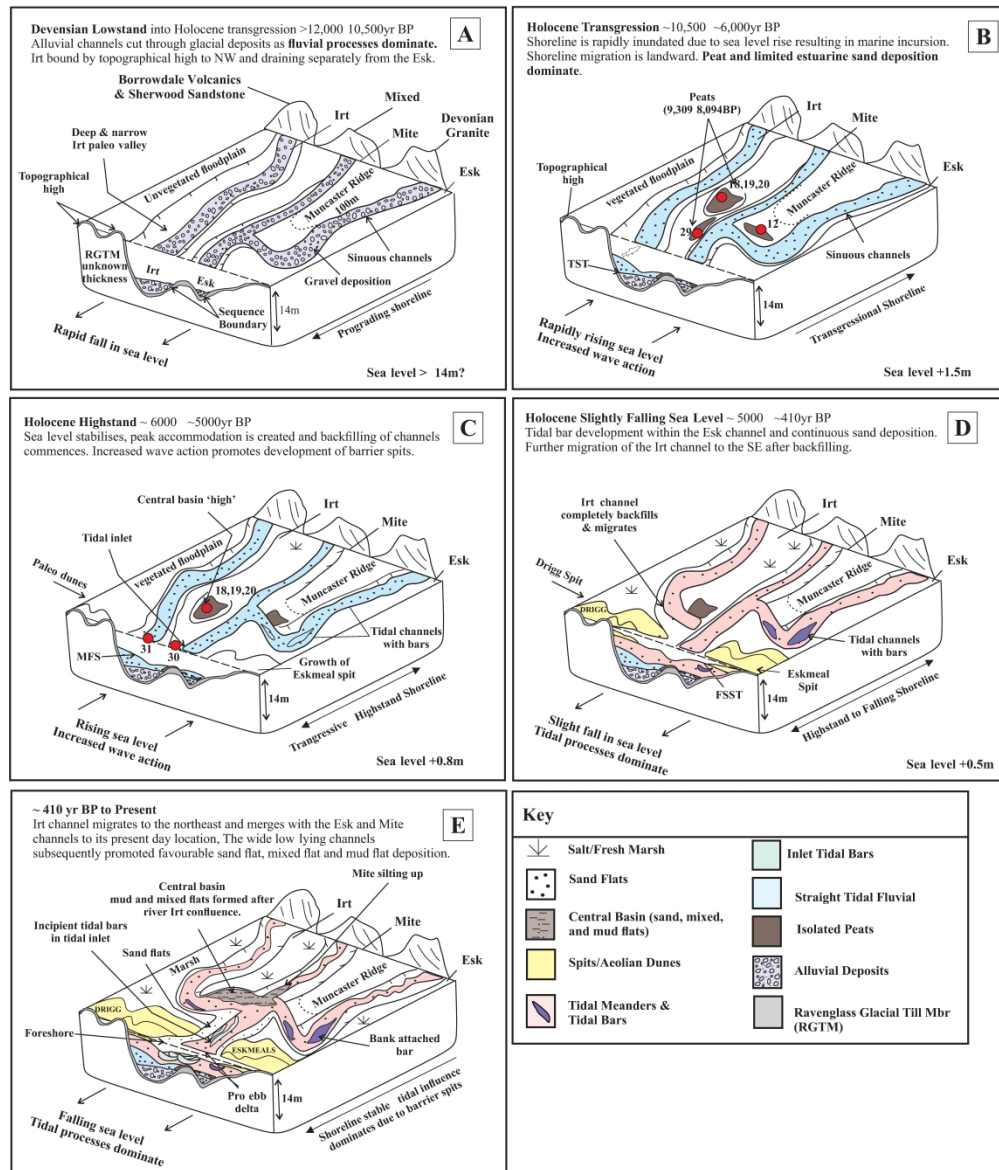


Figure 11. Morphological evolution and corresponding facies of Ravenglass Incised Valley since onset and throughout the Holocene transgression. (a) Incision on the newly exposed post-glacial shelf during the Devensian lowstand (12,000 yrs BP) by a series of sinuous rivers depositing gravel and coarse sands. (b) Holocene transgression which began around 10,500 BP and continued to around 6,000 BP. The initial flooding and landward migration of the shelf promoted peat bed deposition in sheltered areas between the sandy tidal channels. (c) The Holocene Highstand (6,000 to 5000 yrs BP) was a time of sea-level stabilisation and peak accommodation is reached and backfilling of the valleys occurs. The palaeo-Drigg Spit began migrating to the SE. (d) Sea-level begins to fall from 5,000 yrs BP to around 410 yrs BP and the migration of the Drigg Spit and backfilling of the River Irt forced migration to the SE. Tidal sand bars and meandering channel belts accumulated in the River Esk. (e) The River Irt migrates to the NE and joins the Rivers Mite and Esk. The now backfilled, wide and shallow channels have promoted favourable estuarine conditions resulting in the development of the muddy central basin.

291x340mm (600 x 600 DPI)

Table 1. Radiocarbon dating results, showing the samples for each facies association (FA), as well as sediment descriptions, sample depth (m), ^{14}C ages and the associated error (\pm).

<i>FA</i>	<i>Sample Type</i>	<i>Sediment Context</i>	<i>Depth (m)</i>	<i>^{14}C Ages</i>	\pm
Ravenglass Glacial Till Member (RGTM)	Nil	Nil	Nil	Nil	Nil
Alluvial Gravels	Nil	No ^{14}C datable material.	Nil	Nil	Nil
Peats	Peat fragments	Central basin peat beds overlying glacial till. Local depressions with no in-channel deposition.	3.54m	9,309	38
			1.85m	8,416	37
			3.43m	8,094	32
Tidal-Fluvial	Thin white bivalve shells	Medium to coarse grained, moderately sorted sands with shell fragments. Signifies the first sediment deposited within the valley	5.0m	6,971	30
			5.54m	6566	40
				7,948	
Aeolian Dunes	Medium white bivalve shell fragments	Fine to medium grained sediment with rare pebbles and shells.	3.85m	3,910	24
			5.67m	4,341	26
Tidal Meander and Central Basin	Oyster and thin white bivalve shells	Fine grained, poorly sorted sand and mud. Restricted to central basin samples. Upper 1m of sediment contaminated from Sellafield, a nearby nuclear power plant.	1.46m	813	20
			1.48m	733	21
			1.55m	634	26
			1.95m	123	24
Tidal Sand Bar	Thin white bivalve shells	Medium grain sands, moderate to well sorted with shelly horizons.	2.72m	1,229	20
Foreshore	White bivalves and blue oyster shells	Fine to medium grained sand with thicker gravel beds. Located between the Irt and Esk palaeo-channels and potentially a zone of tidal ravinement.	2.58m	9003	
			2.90m	6439	
			1.91m	3629	
			1.91m	3727	
			1.70m	3307	
			1.49m	1890	
Salt & Fresh Marsh	Nil	Nil		Nil	Nil
Upper Flow Regime	Nil	Nil		Nil	Nil

Table 2. Descriptions of Ravenglass Incised valley-fill facies associations (FA) including: thickness (m), correlation lengths (km) texture and sedimentary structures, location and dominant sedimentary processes, relative sea-level and sequence boundaries.

Facies	Thickness (m)	Correlation Length (km)	Texture & Sedimentary Structures	Location & Processes	Sea-Level
Ravenglass Glacial Till Member (RGTM)	0.15-1.0m	Underlies 95% of mapped estuarine stratigraphy.	Grey to reddish in colour, very fine grained (0.063mm), very poorly sorted clay rich till. Commonly chaotic structure with some shell fragments and small clasts.	Inner, central and outer estuary. Glacial to fluvial processes dominate	Highstand?
Alluvial Gravels & Coarse Sands	0.6-3.0m	Up to 0.5 km	Gravel beds with mixed clasts of sandstone, volcanics and granite up to 7cm. Commonly shows sharp contact with Ravenglass Glacial Till Member.	Outer to inner estuary. Alluvial processes dominate	Lowstand to Transgressive. Base of gravels represents sequence boundary.
Estuarine Brown-Black Peats	0.10-1.3m	Up to 0.5 km	Black to dark brown in colour, laminated and well consolidated. Commonly shows sharp contact with Ravenglass Glacial Till Member.	Inner estuary, central basin and tidal inlet. Lowland raised bogs -limited fluvial processes.	Transgressive Central basin shielded.
Salt & Fresh Marsh	0.25-2.0m	Continuous along inner estuarine margins and limits. Up to 3.2 km	Light brown, very fine to fine (0.065-0.125mm) grained laminated silts, poorly sorted and commonly rooted in top 10cm. Overall, fining upwards grain size trend.	Inner estuary, representing the preferential deposition of fine-grained material in an inter- tidal environment. Estuarine Processes dominate.	Highstand to Falling
Tidal-Fluvial Channel Sands	0.2 – 6.5 m	Up to 2.5 km	Fine (0.25-0.125mm) to medium (0.25mm) grained sands, poorly sorted at base with pebbles and moderately to well sorted upwards Flaser beds, silty laminae and clay drapes common. Proximal settings are finer grained with higher heterogeneity.	Inner estuary tidal channel. Estuarine processes dominate.	Transgressive to Highstand
Tidal Sand Bars within Tidal Channels	3.0-5.0m	Up to 0.5 km	Orangey brown, fine (0.25- 0.125mm) to medium (0.25- 0.35mm) grained sandstones, moderate to well sorted with small, disarticulated shell frags. Sands are commonly massive, structures limited to clay drapes no thicker than 10cm. Overall	Inner estuary tidal channel. Estuarine processes dominate.	Highstand

			sands fine upwards.		
Tidal Meander	1.7-3.5m	Up to 1.4 km	Very fine (0.125mm) to medium (0.25mm) grained sands and silts. Commonly interbedded, heterogenous and finer in proximal settings. Commonly fines upwards.	Inner estuary. Estuarine processes dominate.	Highstand to Falling
Tidal Sand Flats	Up to 1.2m	Up to 1 km	Fine to medium grained (0.125-0.25mm), well sorted sands, bioturbation near central basin channel.	Foreshore and backshore. Marine processes dominate on foreshore and estuarine on backshore.	Highstand to Falling
Aeolian Dunes (Barrier Spits)	Up to 5.5m	Drigg and Eskmeal Spits occupy a surface area of 3.1 km ² and 2.76 km ²	Light brown, med (0.25mm) to coarse (0.5mm) grained, moderate to well sorted sands. Small pebbles present with charcoal fragments.	Foreshore and backshore. Marine wave action & longshore drift forming spit. Wind processes dominate.	HSST-FSST

1 Stratigraphy and sedimentary evolution of a modern macro-tidal incised 2 valley – an analogue for reservoir facies and architecture

3 Claire McGhee^{1#}, Dahiru Muhammed², Naboth Simon², Sanem Acikalin¹, James E. P. Utley², Joshua
4 Griffiths^{2,3}, Luke Wooldridge^{2,3}, Iris T. E. Verhagen², Cees van der Land¹, Richard H. Worden^{2*}

5 1. *School of Natural and Environmental Sciences, Newcastle University, NE1 7RU, UK*

6 2. *School of Environmental Sciences, Liverpool University, L69 3BP, UK*

7 3. *BP Exploration, Chertsey Road, Sunbury-on-Thames, Middlesex, TW16 7LN, UK*

8
9 # contact author: C.A.McGhee2@newcastle.ac.uk

10 * research project lead and contact author: r.worden@liverpool.ac.uk

11 Abstract

12 Incised valley fills are complex as they correspond to multiple sea-level cycles which makes
13 interpretation and correlation of stratigraphic surfaces fraught with uncertainty. Despite numerous
14 studies of the stratigraphy of incised valley fills, few have focused on extensive core coverage linked
15 to high fidelity dating in a macro-tidal, tide-dominated settings. Here, we have drilled nineteen
16 sediment cores through the Holocene succession of the macro-tidal Ravenglass Estuary in northwest
17 England, UK. A facies and stratigraphic model of the Ravenglass incised valley complex was
18 constructed, to understand the lateral and vertical stacking patterns relative to the sea-level changes.
19 The Ravenglass Estuary formed in five main stages. First, incision by rivers (~11,500 to ~10,500 yrs
20 BP) cutting through the shelf during lowstand, which was a period of fluvial dominance. Secondly, a
21 rapid transgression and landward migration of the shoreline (10,500 to 6,000 yrs BP). Wave action
22 was dominant, promoting spit formation. The third stage was a highstand at ~6,000 to ~5,000 yrs BP,
23 creating maximum accommodation and the majority of backfilling. The spits narrowed the inlet and
24 dampened wave action. The fourth stage was caused by a minor fall of sea-level (~5,000 to ~226 yrs
25 BP), which forced the system to shift basinward. The fifth and final stage (226 yrs BP to present)
26 involved the backfilling of the River Irt, southward migration of the northerly (Drigg) spit and
27 merging of the River Irt with the Rivers Esk and Mite. The final stage was synchronous with the
28 development of the central basin. As an analogue for ancient and deeply buried sandstones, most of
29 the estuarine sedimentation occurred after transgression, of which the coarsest and cleanest sands are
30 found in the tidal inlet, on the foreshore and within in-channel tidal bars. The best-connected (up to
31 1km) reservoir-equivalent sands belong to the more stable channels.

32
33 Keywords: Incised-valley, Ravenglass, estuary, tide-dominated, connectivity, sandstone reservoir
34 quality, sequence stratigraphy

35

36 **1. Introduction**

37 Incised valleys form as a result of basinward migration of the shoreline, inducing exposure of the
38 shelf and promoting enhanced fluvial incision within the lower reaches of the coastal valleys. The
39 valley fills during landward migration of the shoreline and contains the most complete record of
40 lowstand, transgression and subsequent highstand deposition (Zaitlin *et al.*, 1994). The stratigraphic
41 expression of the deposits within the valley can promote sediment preservation that can result in
42 highly economical oil and gas reservoirs and storage sites for carbon dioxide for CCS projects (Salem
43 *et al.*, 2005; Hein, 2015; Wang *et al.*, 2019; Meng *et al.*, 2020). The understanding of reservoir facies
44 and stratigraphic architecture of incised valley-fills is also critical for predicting a field's recoverable
45 hydrocarbon potential (Hampson *et al.*, 1999; Slatt, 2013; Wang *et al.*, 2019) and reducing overall
46 risk. The valley deposits are unique in that they represent the creation of accommodation space by one
47 process (migration of shoreline) and the infill by a range of processes (wave, tide and fluvial) (Boyd
48 *et al.*, 2011). In many modern and ancient examples of incised valleys, the sediment fill is typically
49 composed of coarse-grained fluvial and alluvial beds at the valley base. Subsequent transgression and
50 sea-level highstand result in estuarine and marine sedimentation, of which the former appears to be
51 the most common volumetrically (Allen and Posamentier, 1993; Chaumillon *et al.*, 2010; Garrison
52 and Bergh 2006; Willis and Gabel, 2001). Estuarine sedimentation within the valley is complex in
53 that the deposits are the product of river, tide and wave action causing a tripartite zonation of facies
54 that corresponds to net bedload transport (Boyd *et al.*, 2011). Compound filling (corresponding to
55 multiple phases of sea-level cycles) of such valleys results in complex architecture, resulting in
56 extensive amalgamation of stratigraphic surfaces (Zaitlin *et al.*, 1994). Widely adopted conceptual
57 facies models and stratigraphic frameworks have been developed to explain and predict the
58 distribution of sediment within incised valleys during transgression (Allen and Posamentier 1993;
59 Dalrymple *et al.*, 1992; Heap *et al.*, 2004; Zaitlin *et al.* 1994). A recent study by Wang, *et al.*, (2020)
60 demonstrated that 87 Quaternary incised valley fills showed similar stratigraphic organisation
61 comparable to the classic conceptual models (Dalrymple *et al.*, 1992b; Allen & H. W. Posamentier,
62 1993; Zaitlin *et al.*, 1994; Heap *et al.*, 2004; Virolle *et al.*, 2019) but displayed significant variability
63 in the stratigraphic architecture of valley fills, related to continental margin type, inherited
64 topography, river size, catchment area and shoreline hydrodynamics. Depending on the dominant
65 hydrodynamics at the estuary mouth, two end-members have been recognised (Dalrymple *et al.*,
66 1992). Wave-dominated estuaries are typically described as possessing a tripartite zonation of facies;
67 a barrier spit at the estuarine mouth, tidal inlet, a sheltered muddy central basin and a bayhead delta.
68 In tide-dominated systems, the marine sand body is made up of elongate tidal bars in the inlet and the
69 mouth. The meandering channel belt in tide-dominated settings is the equivalent to the central basin in

70 the wave-dominated models. Typically, the inner estuarine facies above the sequence boundary in
71 wave-dominated settings can be very muddy compared to sandy facies in the tide-dominated settings.

72 Despite a vast amount of literature regarding the stratigraphy of incised valley fills, few have focused
73 on high resolution core coverage coupled with high fidelity dating within a macro-tidal tide-
74 dominated setting. The Cobequid Bay–Salmon River estuary, located in the Bay of Funday (Tessier,
75 2012), is arguably one of the most cited modern examples of a tide-dominated valley fill (Dalrymple
76 & Zaitlin, 1994) and represents the basis for the Dalrymple *et al.*, (1992) classic conceptual model.
77 The Gironde Estuary in France is also another commonly cited tide-dominated valley fill (Allen and
78 Posamentier 1993; Fenies and Tastet 1998; Virolle *et al.* 2019). Ravenglass is a scaled down version
79 of many modern estuaries discussed in the literature, covering an area of 5.6 km² (Chaumillon *et al.*,
80 2010a; Menier *et al.*, 2010). The Gironde Estuary (SW France) and the tide-dominated paleo-
81 Changjiang in China have drainage basins that cover approximately 75,000 km² (Allen and
82 Posamentier, 1993) and 1.8×10^6 km² (Hori *et al.*, 2001) respectively. Despite differences in scale
83 and sediment supply, the three estuaries possess similar morphologies.

84 The lateral and vertical stacking patterns of the Holocene deposits of the Ravenglass estuary,
85 northwest England, UK were investigated, in order to model facies distributions within a tide-
86 dominated incised valley. According to Zaitlin *et al.*, (1994), the deposits have formed a single,
87 simple-fill in that most of the deposits correspond to one cycle of sea-level fall and rise during the
88 Holocene (Lloyd *et al.*, 2013). The Ravenglass incised valley is a relatively small, modern day macro-
89 tidal estuary with a multi-tributary system that extensive interpretation of the surface and shallow
90 subsurface sediment (Griffiths *et al.*, 2018; Wooldridge *et al.*, 2018, 2019). Here, the study will
91 examine the complete sedimentary in-fill of the Ravenglass valley, produce detailed facies
92 descriptions and create high resolution correlations linking shoreline migration to style of
93 sedimentation.

94 This study aims to address the following research questions, in order to summarise the evolution of
95 the Ravenglass Estuary incised valley-fill:

- 96 1. What is the stratigraphic organisation of infill for the Ravenglass Estuary?
- 97 2. What are the architectural elements of the infill for the Ravenglass Estuary?
- 98 3. What is the morpho-sedimentary evolution of the valley?
- 99 4. Is lateral and vertical correlation of facies possible over 100 m to 1,000 m scales?
- 100 5. How does the Ravenglass incised valley-fill compare to current stratigraphic models?

101 2. Geological Setting & Hydrodynamics

102 The Ravenglass Estuary is located in Cumbria, England (Fig. 1a), west of the Lake District mountains
103 (maximum elevation of 980 m at Scafell Pike). It is one of the most natural and least developed

104 estuaries in the UK, with little industry and virtually no artificial coastal defences. The estuary lies on
105 relatively flat low-lying coastal plain, occupying an area of 5.6 km², of which approximately 80 % is
106 intertidal (Bousher, 1999; Lloyd *et al.*, 2013; Wooldridge *et al.*, 2017a; Griffiths *et al.*, 2018, 2019;
107 Wooldridge *et al.*, 2018). The estuary is a mixed energy, macrotidal system with a mean spring tidal
108 range of > 7 m, leaving the estuary nearly fully drained at low tide. The estuary is fed by three main
109 rivers, the Irt, Mite and Esk. The River Irt flows at 3.4 m³/s⁻¹ and the River Mite flows at 0.4 m³/s⁻¹
110 (Bousher, 1999) The River Esk has an average flow rate of 4.2 m³/s⁻¹ (broadly similar with the River
111 Irt) with suspended sediment concentrations of 20-70 gm⁻³ during spring tides and 5-20 gm⁻³ during
112 neap tides (Assinder *et al.*, 1985). These westward-draining rivers cut through the steep hinterland
113 topography of the English Lake District and meet at a point of confluence creating a single tidal
114 channel (Fig. 1b). Restriction in the tidal inlet size can be attributed to the formation of the Drigg
115 barrier spit to the northwest and the Eskmeal barrier spit to the southeast (Fig. 1b). Strong tidal
116 asymmetry occurs due to the shallow bathymetric nature and short length of the estuary (Kelly *et al.*,
117 1991). Modern surface facies from the Ravenglass estuary consist of gravel, tidal flats, fluvial tidal
118 bars (alternate bars) and dunes, tidal-inlet, backshore, foreshore and pro-ebb delta (Wooldridge *et al.*,
119 2017b; Griffiths *et al.*, 2018; Simon *et al.*, 2021).

120 The Ravenglass Estuary is underlain to the west of the Lake District Boundary Fault by Triassic
121 Sherwood Group sandstones, and to the east by Devonian Eskdale Granites, Ordovician Borrowdale
122 Volcanics and the Cambrian Skiddaw Group. The River Irt drains Borrowdale Volcanic Group
123 andesites and Sherwood sandstones whereas the River Esk drains the Eskdale granite and
124 granodiorite. The minor River Mite drains Eskdale granite and granodiorite and Borrowdale volcanic
125 rocks.

126 **3. Quaternary Geology**

127 Western Cumbria has been affected by periodic Quaternary glacial advance and retreat (Royd, 2002;
128 Merritt & Auton, 2000), with the most recent event occurring during the Mid to Late Devensian
129 (MLD), between 28,000-13,000 yrs BP (Moseley, 1978). During the MLD, Ravenglass lay in an ice-
130 sheet convergence zone, fed by ice from both Scotland to the north and the Lake District to the east.
131 Ice flow directions have been interpreted from the distribution of erratics (granite and greywackes
132 from the Southern Uplands of Scotland) and drumlin orientation, which support the interpretation of
133 Scottish Ice impinging on the Cumbrian coastline (Merritt & Auton, 2000). The evolution of the
134 Cumbrian coastline and resulting sediment deposits have been greatly modified by post-glacial
135 processes and changes in relative sea-level linked to spatially variable glacio-isostatic rebound (Zong
136 & Tooley 1996). According to the lithostratigraphic and biostratigraphy study of central Cumbria, and
137 specifically Ravenglass, the area underwent a sea-level highstand of approximately +2.3 m Ordnance
138 Datum (OD) during the Late Devensian between 17,000 and 15,000 yrs BP. From 15,000 to 11,500

139 yrs BP, a rapid fall in sea-level below -5 m OD (modelled up to -30m) occurred as glacio-isostatic
140 rebound exceeded global sea-level rise. After the period of incision, a rapid marine transgression
141 began in the Early Holocene between 11,500 to 6,000 yrs BP, followed by a stabilised highstand,
142 estimated at +2 m OD with a gradual fall until present (Lloyd et al., 2013) (Fig.2).

143 **4. Samples & Methods**

144 To construct a facies architecture model of the Ravenglass Estuary Holocene sedimentary sequence,
145 information on the age and depositional environments of the sediments was investigated. To do this,
146 radiocarbon dating and detailed core descriptions from 19 cores were undertaken.

147 **4.1 Core Acquisition**

148 Nineteen cores were drilled through the Holocene succession as far as the Ravenglass Glacial Till
149 Member, under tender by Geotechnical Engineering Ltd. All sites were subject to an initial desk study
150 to estimate depth to glacial till based on previous reports and publications (Assinder et al., 1985;
151 Kershaw *et al.*, 1990; Halcrow Group, 2013; Coast and Area, 2015). All sites were subject to
152 environmental impact assessment in conjunction with Natural England; several sites in, and around,
153 the estuary required the presence of an independent ecologist to ensure there was no damage to
154 protected species such as natterjack toads and great crested newts. Due to more than 100 years of
155 weapons testing from the Ministry of Defence-owned Eskmeals firing range (located on the southern
156 spit with heavy-artillery firing out into the East Irish Sea) much of the beach and tidal inlet was
157 flagged as high-risk for unexploded ordnance (UXO). The risk of UXO was mitigated by Lankelma
158 Ltd who appraised each foreshore and pro-ebb delta site with a magnetometer probe mounted on a
159 wide-tracked vehicle (Fig. 4d) immediately before coring. Core acquisition had to be timed around
160 periods of low tide and at least two cores were collected at each site. Cores were acquired using either
161 a Geotechnical 'P60' Rotary rig or a Geotechnical "Pioneer" rotary rig. The Pioneer rig is a light-
162 weight percussion rig that was used on soft substrates, such as mudflats (Fig. 4c) and vegetated tidal
163 bars (Fig. 4a). The P60 is a heavier rotary rig which was used on hard substrates such as sandflats
164 (Fig. 4b) and in areas of uneven land surface, such as the upper reaches of the Esk Estuary flood plain,
165 as it is capable of operating on slopes of up to 45 degrees. The retrieved cores were 12 cm in diameter
166 retained in a semi-rigid plastic liner and transported back to the University of Liverpool for
167 subsequent analysis.

168 **4.2 Core Descriptions**

169 The 19 sediment cores were sliced and photographed wet, and after air-drying. Detailed logging of
170 each core was undertaken, wet and then dry, at a scale of 1:5. Facies were described in terms grain
171 size, sorting, colour, sedimentary structures, bed thickness, presence of roots and shell fragments,
172 bioturbation index and type of bioturbation.

173 **4.3 Radiocarbon Dating (^{14}C)**

174 Nineteen radiocarbon analyses were undertaken under contract by the Chrono Centre, which is part of
175 Queen's University of Belfast, in Northern Ireland, UK. Samples of shell fragments and organic
176 matter were taken from the cores as they were logged. The precise depth and type of material was
177 carefully recorded (Table 1).

178 The shell fragments used for dating were identified as bivalves, such as oysters. Shells were classified
179 as being thin or thick specimens. It was recognised that thick samples may have been able to
180 withstand erosion from their initial site of deposition, followed by subsequent re-deposition; thick-
181 shelled samples are therefore more liable to anomalous ages than thin-shelled samples. Organic matter
182 subject to dating included leaf-bearing peat.

183 Samples from the top 1 m of sediment were not subject to radiocarbon dating since they were
184 considered to be at risk of contamination from radionuclides, including ^{14}C , released accidentally
185 from the Sellafield (previously known as Windscale) nuclear reprocessing site, 15 km north of
186 Ravenglass, since its inception in 1947.

187 **5. Post-glacial palaeo-topography**

188 All available data related to the depth of the Ravenglass Glacial Till Member (RGTM) throughout the
189 Ravenglass Estuary are collated in Figure 3. Data from cores published by Merritt and Auton (2000)
190 and a core from the British Geological Survey (BGS, 1939) data repository were also plotted on the
191 palaeo-topographical map. The map further incorporates glacial till outcrop locality information from
192 Ravenglass (Griffiths et al., 2019). Based on the 28 spot depths to glacial till, a tentative palaeo-
193 topographical map of the Ravenglass area has been drafted, prior to valley being infilled (Fig. 3).

194 The palaeo-Irt, in the northwest of the area, had a steep northwest-side with a relief of ~ 22 m. South-
195 east of palaeo-Irt, the land surface rose up, by ~ 12 m, with a local "high" in the area currently
196 occupied by the central basin of the present-day estuary (Fig. 3). On this basis, the palaeo-Irt flowed
197 directly into the Irish Sea rather than deviating to the southeast and joining the palaeo-Esk. The initial
198 separation of the palaeo-Irt from the palaeo-Esk is supported by historical map information that shows
199 that the Irt only merged with the Esk at approximately 270 yrs BP. A map by Speed from the year
200 1610 ME (Speed, 1610) shows the Irt flowed directly into the Irish Sea, while a map by Thomas
201 Donald from the year 1774 ME (Donald, 1774) shows the estuary had adopted the current
202 geomorphology with the River Irt deviating to the southeast and joining the Rivers Esk and Mite.

203 Based on the mapped contours to the glacial till, the palaeo-Esk followed the outline of the present-
204 day River Esk, in that it deviated to the north-west and joined the much smaller River Mite (Fig. 3). It
205 was previously suggested that the palaeo-Esk flowed directly into the Irish Sea (Halcrow Group,
206 2013) but there seems to be no evidence to support this interpretation. Moreover, there is

207 archaeological evidence (signs of a Neolithic flint napping factory, possibly as old as 9,000 yrs BP;
208 (Bonsall *et al.*, 1989; Clare *et al.*, 2001)) proving the existence of the Eskmeals spit immediately after
209 the glacial retreat, supporting our interpretation of the trajectory of the palaeo-Esk.

210 **6. Facies analysis and interpretation**

211 In this section, results are presented from field observations, aerial photography, core analysis in the
212 form of sedimentary logs, facies characterisation and radiocarbon dating, in order to assess the infill
213 of the incised valley and to establish whether correlation over hundreds to thousands of meters is
214 possible. This work also aims to build on the surface and 1 m core studies by Wooldridge *et al.*
215 (2018).

216 The total thickness of the post-glacial sedimentary infill for Ravenglass Estuary is up to 9m, close to
217 the estuary mouth, thins to the east (landward) to between 4 m and 6 m in the cores (Fig. 6, 7, 8 and
218 9). A total of nine facies were identified in the core and are illustrated in Figure 4 and listed in Table
219 2.

220 **6.1 Ravenglass Glacial Till Member (Seascale Glaciogenic Formation) (Inner and** 221 **Outer Estuary)**

222 The Ravenglass Glacial Till Member (RGTM) underlies the majority of the Ravenglass estuary and is
223 present in all cores except 18 and 27 (Figs. 3 and 7). The till forms part of the Seascale Glaciogenic
224 Formation (Merritt and Auton, 2000). The grey-brown, stiff, matrix-supported, silty clay represents
225 the lowest part of the stratigraphy in many of the cores and also outcrops as knolls throughout the
226 estuary. The till is poorly sorted and displays a chaotic structure with rare sedimentary and meta-
227 sedimentary clasts and rare shell fragments. The till varies in thickness across the estuary based on
228 core data (between 0.2 and 1.0 m) and shows a sharp contact with the overlying facies. The
229 distribution of glacial till within the valley is probably a product of the movement of meltwaters from
230 the retreating and advancing ice-sheets to the north northwest, that focussed around the Esk and
231 present-day foreshore (Delaney, 2003). It has been suggested that the tills are a result of proglacial
232 lakes fed by glacial meltwaters during the Main-Late Devensian (MLD) (Merritt & Auton, 2000). The
233 older, Late Devensian ('late glacial') set of tills, which occur sporadically around the Cumbrian coast,
234 were formed during, and shortly after, retreat of MLD ice. The top of the RGTM represents the
235 sequence boundary.

236 **6.2 Alluvial Gravel & Coarse Sands**

237 The gravel and coarse sands (cores 1, 3, 12, 27, 28, and 31; Figs. 6, 7 and 9) commonly overlie the
238 RGTM and vary in thickness (0.6 to 3.0 m). The gravels and coarse sands can be correlated over
239 distances of 0.5 km in the outer estuary (Fig. 9). The clasts range from 3 to 7 cm in size, are angular to
240 sub-angular and are sedimentary, meta-sedimentary and igneous, suggesting the source is

241 predominantly from the catchment area. Poor sorting, angularity and the absence of shell fragments
242 suggest that the gravels are of fluvial-alluvial origin. Radiocarbon dating was not possible due to the
243 absence of shells and peat. The occurrence of gravel beds beneath the estuarine deposits implies that a
244 fluvial-alluvial system extended ~15-20 km further west (seaward) than the present-day coastline.
245 Merritt & Auton (2000) have suggested a relative sea-level fall of -30 m below ordnance datum at
246 ~10,200 yrs BP which could have resulted in the deposition of the gravels. The base of the fluvial
247 gravels represents the sequence boundary within the valley.

248 ***6.3 Estuarine Brown-Black Peats***

249 Brown-black peat (cores 12, 18, 19, 20, 29 and 32; Figs. 6, 8 and 9) is rich in indistinct, probably
250 deciduous, leaves and other woody plant material and is likely terrestrial in origin. It also contains
251 some silt and is well consolidated. Peat thickness varies across the estuary between 0.1 and 1.3 m
252 (Figs. 7, 8 and 9). Peat occurs directly on top of the glacial till at sites where fluvial-alluvial gravel
253 and coarse sands are absent. In the inner estuary, the peats can be correlated over distances of 0.5 km
254 but are commonly laterally discontinuous. This facies typically displays a sharp contact with the
255 overlying estuarine sands and underlying till or gravel and is mostly concentrated in the central basin
256 and in the Esk channel.

257 As shown by the radiocarbon dating, the peat beds are the oldest Holocene sediments from the valley-
258 fill that can be dated, since the underlying fluvial-alluvial gravels do not contain organic matter and
259 shells. The peats are between $8,094 \pm 32$ and $9,309 \pm 38$ BP in age and conform to the Holocene
260 transgression (Fig. 2; table 1).

261 Considering their variable distribution, location between channels and contact with the fluvial
262 deposits below, the peats represent the first deposits of the valley during the Holocene transgression.
263 The transition from glacial-fluvial deposits below the peats, indicates that some areas of the valley
264 were in isolated and sheltered locations of poorly drained topographical depressions (between palaeo-
265 channels).

266 ***6.4 Salt and Fresh Marsh***

267 Salt and fresh marsh sediment is present in cores 1, 3, 7, 8, and 10 (Fig. 6). Commonly distributed
268 throughout the inner estuary and estuary limits, the marsh-related sediment is typically composed of
269 planar laminated, poorly sorted, very fine silts and clays with vegetated tops, in the form of roots.
270 Marsh thickness varies across the estuary from 0.25 to 2.0 m, with the thickest deposits at the
271 proximal channel margins (Fig. 6), where they are continuously correlatable over 3.2 km.

272 Salt and fresh marsh commonly represent the final stages of the levelling of marine coastal plains and
273 the presence of marsh above the meanders and sand bars in cores 1, 3, 7, 8, and 10 implies a phase of
274 abandonment as rivers have migrated. Salt and fresh marsh sediment is either linked to transgression

275 or regression; here the stratigraphic context leads to the interpretation that the salt and fresh marsh
276 sediment represents falling sea level (regression).

277 **6.5 Sand-Dominated Sediments**

278 The sand-dominated sediment has been subdivided into a variety of sub-facies from geographic and
279 stratigraphic positions, based on grain size, sorting, sedimentary structures, presence of shell and peat
280 fragments, and presence of minor silt and mud laminae. Five sand-rich facies have been identified for
281 the Ravenglass valley fill: tidal-fluvial deposits, tidal sand bar deposits, tidal meander deposits, outer
282 estuary-shoreface deposits and dune deposits.

283 **6.5.1 Tidal-Fluvial Channel Sands**

284 The tidal-fluvial sand facies (present in all cores except 28; Figs. 6, 7, 8 and 9) are present in most
285 cores and throughout the estuary. They represent a landward thinning wedge of sandy estuarine
286 sediment that, in terms of measured thicknesses in core (0.2 -6.3 m), makes up less than a third of the
287 Holocene valley-fill. The facies are composed of fine-medium (0.125-0.25 mm) grained sands with
288 shell debris at the base and higher concentrations of silty-mud laminae in the inner estuary. This
289 sandy facies commonly fines upwards, for example in cores 7, 8, 10 and 12. Pebbles and clay drapes
290 are common at the base in the inner estuary sands and reworked peat clasts are common, particularly
291 in the Irt channel and outer estuary. With a radiocarbon age of $7,848 \pm 40$ - $6,827 \pm 31$ yrs BP, they
292 represent the first estuarine sands within the valley.

293 The presence of tidally-influenced fluvial sands above the RGTM, suggests that these facies were the
294 first estuarine sand to be deposited within the valley during transgression. Thus, the tidally influenced
295 fluvial sands were deposited as aggrading, transgressive- to highstand-facies which onlap the low-
296 stand fluvial deposits during landward migration of the shoreline. The shelly material (dominated by
297 disarticulated bivalves) mixed with the tidal-fluvial sand implies that the sand possibly had a
298 dominant marine source that was reworked by tidal currents, also suggested by Bousher (1999).

299 **6.5.2 Tidal Sand Bars within Tidal Channels**

300 The tidal sand bar facies (cores 7, 8, 12, 25 and 26; Figs. 6, 8 and 9) are present above the RGTM and
301 peat beds and are deposited along the sinuous section of the Rivers Esk and Irt. Tidal sand bar facies
302 are composed of fine to medium (0.125-0.35 mm) grained sands, that are moderately to well sorted
303 with horizons of small, disarticulated shell debris. The tidal sand bars can be correlated up to 0.5 km
304 in the tidal channels. Pebble beds with shell debris are common at the base and clay drapes are
305 preferentially observed towards the top. Overall, the facies show a significant fining upwards profile,
306 at the multi-metre scale, from pebbly gravel, through medium grained sand capped with laminated silt
307 and mud that is typically vegetated after abandonment.

308 The deposition of the sand bars symbolises the time when sea-level stabilised, with the development
 309 of channel banks. The disarticulated shelly and pebble surfaces most likely reflect internal erosion
 310 and migration surfaces within the bar.

311 **6.5.3 Tidal Meander (Inner Estuary)**

312 Tidal meander sediments (cores 1, 3, 10, 18, 19 and 20; Figs. 6, 7 and 8), are restricted to the most
 313 proximal environments and are composed of planar to slightly inclined lamination, alternating very
 314 fine to medium (0.125- 0.250 mm) grained sand and silt. Flaser bedding occurs in the mid to upper
 315 sections of the facies with localised clay drapes. Silt interbeds are common in most proximal settings
 316 and they are capped with root-rich fresh marsh. The heterolithic, silt-rich strata are indicative of
 317 floodplain development associated with a meandering river system; these facies are restricted to the
 318 top 3 m of upper estuary cores because it only developed once sediment had been stabilised by
 319 vegetation. The tidal meander sediments can be correlated 1.4 km downstream in the inner estuary.

320 **6.5.4 Tidal Sand-Flat (Outer Estuary to Upper Wave-Dominated Shoreface)**

321 The outer estuary zones represented by the foreshore, tidal inlet and backshore sediments are medium
 322 grained (0.25 mm), well sorted sands and show rippled to planar laminations; they are interpreted to
 323 represent tidal flats (cores 27, 28, 29, 30 and 31; Fig. 9). This type of sediment is currently present in
 324 the foreshore beach and main tidal channel bank sediments and can be correlated up to 1 km over the
 325 foreshore. Close to the main tidal channel, the sands form superimposed low-amplitude dunes that are
 326 constantly remobilised by tidal currents. Therefore, in the cores, these relatively coarse grained,
 327 rippled to planar laminated sediments are interpreted to result from the progradation of sands at, or on
 328 either side of, the mouth of the tidal inlet.

329 It is noteworthy that there is an absence of well-developed tidal bars in the main tidal channel of the
 330 modern Ravenglass Estuary; this is due to the relatively limited modern supply of sand-rich sediment
 331 from the rivers and the constant remobilisation by tidal currents. The restricted sand-supply and
 332 constant remobilisation probably lasted throughout the Holocene resulted in limited occurrence of
 333 tidal bars in the sediment cores. The tidal inlet itself lacks modern accommodation for the
 334 development of well-developed bars (Fig. 1b).

335 **6.5.5 Aeolian Dunes (Barrier Spits to Outer Estuary)**

336 The aeolian deposits (core 28; Fig. 9) are composed of medium to coarse grained (0.25-0.5 mm),
 337 moderate to well-sorted sands, with small pebbles and charcoal fragments (~ 3 cm) which are
 338 common throughout. The aeolian facies only occurs in the top five metres of one core, on the current
 339 Drigg Spit; the base of the aeolian deposits occurs after $3,910 \pm 24$ yr BP (Fig. 9; Table 2). The
 340 modern vegetated aeolian dunes, known as the Drigg Spit to the northwest and Eskmeal Spit to the
 341 southeast, separate the foreshore and the backshore, here defined as sand-rich shore to the main part
 342 of the inner estuary. The dune deposits subsequently constrict the tidal inlet.

7. Discussion

7.1 Controls on Facies Organisation

The controls on facies organisation of incised valley-fills are a function of the balance between sea-level rise and sediment supply, coupled with incised valley area and hydrodynamics (Garrison & Bergh, 2006; Davis & Dalrymple, 2010; Virolle *et al.*, 2019, 2020). The dominant controls on the Holocene facies expression and organisation of the Ravenglass valley-fill mostly conform to those outlined in the wave to tide-dominated estuarine models by Allen and Posamentier (1993) and Dalrymple *et al.* (1992). Differences to these idealised models are expected due to local variations in estuarine settings, relative sea-level, climate, tectonics and scale. The Ravenglass valley owes its existence to the Devensian lowstand, and its fill to Holocene transgression and highstand. A complete fill through the valley (> 9 m) shows that the sequence boundary is characterised by a gravel lag cutting through pre-existing till deposits. In the outer estuary (Fig. 2) the gravels are followed by coarse grained, cross-bedded sands that generally coarsen upwards with some rare heterolithic bedding in the form of clay drapes (Fig. 9, cores 27, 29, 29). In the inner estuary (Fig. 2) the sands fine upwards into rhythmic heterolithic bedding and are commonly capped by marsh (Fig. 6, cores 1, 3, 7, 8 and 10) The aeolian dunes are not considered as part of the fill due to their low preservation potential. The evolution of this filled and associated hydrodynamics are discussed below.

7.2 Process-Based Classification of Ravenglass Incised Valley

The present-day surface of the Ravenglass valley-fill generally shows the typical tripartite zonation of facies with coarse sandy barrier spits/inlet, weakly developed central basin tidal (mud) flats and the common presence of sand bars towards the head of the estuary in the tidal inlet and the Irt and Esk arms systems (Fig. 1); this zonation is normally indicative of wave dominated systems (Dalrymple *et al.*, 1992). The central basin of Ravenglass estuary is weakly developed as it is limited to the extensive mud and mixed tidal flats that have been deposited around the confluence zone of the Rivers Irt and Mite. In terms of timing, these mud and mixed mud flats are fairly recent, dating $\sim 813 \pm 20$ yrs BP in the River Irt (Fig. 8). The deposition and expansion of the mud and mixed flats is also likely attributed to the development of the turbidity maximum at the point of river confluence, a zone containing higher proportions of suspended sediment (Geyer, 1993; Sanford *et al.*, 2001; Jalón-Rojas *et al.*, 2015). Inhibition of sediment transport via flood currents can also promote extensive central basin muds to form, such as the muds present in the funnel of the Gironde Estuary in SW France (Allen & Posamentier, 1993; Wells, 1995; Virolle *et al.*, 2019, 2020). However, along the axis of the estuary (Fig. 10), grain size tends to increase seaward and decrease landward, suggesting that, throughout the valley fill, the flood currents promoted fluvial sediment transport rather than inhibited it.

377 The overall fill of Ravenglass can be categorised as a mixed tide/wave dominated system since the
378 onset of the Holocene to the present day. Ravenglass estuary possesses some morphological features
379 like that of wave-dominated estuaries, such as barrier spits and a central basin, however a strong tidal
380 signature of the facies prevails. The presence of the tidal inlet, tidal sand bars and tidal flats within the
381 system (Figs. 1b, 6, 7, 8 and 9) and the lack of a well-developed muddy central basin or bayhead
382 delta, strongly support the interpretation of tide-dominance with wave influence. During the initial
383 filling of the valley, tidal range was potentially limited compared to the >7m present-day macro tidal
384 range, and fluvial and wave action were stronger. The reduced tidal range at the start of estuary filling
385 is supported by the presence of the wave-influenced coarse-grained cross-bedded sands above the
386 sequence boundary in the outer estuary (Fig. 9, cores 27, 28 and 29). In the outer estuary, the sands
387 above the sequence boundary show some evidence of tidal influence suggesting the tidal channels
388 have always been restricted from wave action (Fig. 6, cores 1, 3 and 10). As the Drigg and Eskmeal
389 spits were migrating to the southeast and northwest, ultimately narrowing the inlet, wave penetration
390 within the valley was likely decreasing and tidal range increasing. This is evident from the transition
391 of the wave-influenced coarse-grained sands to the medium grained clay draped sands present in cores
392 27, 29 and 31 at around -3m OD (Fig. 9) and the development of sand flats above. Based on the
393 coastal processes classification scheme by Ainsworth *et al.*, (2011), Ravenglass valley was initiated as
394 a dominantly fluvial system that dissected the coastal plain with the deposition of the gravels (cores 1,
395 3, 12, 27, 28, and 31; Figs. 6, 7 and 9). Landward migration of the shoreline due to rising sea-level
396 (Fig. 2) and the formation and migration of the Drigg and Eskmeal barrier spits (Fig. 9, core 28)
397 represents a transition from a fluvial-dominated to wave-dominated system with secondary tide and
398 fluvial influence. Possibly during and after the formation of the barrier spits and tidal inlet, tidal
399 processes became dominant, resulting in extensive estuarine mud flats in the outer estuary (Figs. 7
400 and 8, cores 18, 19, 20, 25, 26) and sand flats within the inner estuary (Fig. 9, cores 27, 28, 30 and
401 31).

402 Throughout the Holocene, valley filling processes have been somewhat segregated in that, wave
403 dominated processes have controlled deposition in the foreshore and tidal processes have dominated
404 in the tidal inlet and tidal channels. The progradation of the present-day tidal inlet is likely to cut
405 stratigraphically deeper and be less susceptible to later transgressive ravinements. This could lead to
406 wave processes being under-represented in the sedimentary record since the tidal inlet is preferentially
407 preserved. The majority of the valley fill of Ravenglass commenced at the end of the Holocene
408 transgression (Fig. 1b) and tidal ravinement could have also contributed to the lack of wave-
409 dominated facies present in the Ravenglass estuary cores (Fig. 9, cores 27, 28, 29).

410 **7.3 Correlation and Architectural Elements**

411 The lateral and vertical distribution of the different facies identified from the core logs have here been
412 correlated relative to the RGTM as it occurs throughout most of the inner and outer estuary (Figs. 6,

413 7, 8 and 9). Overall, the architecture of the Ravenglass valley fill, above the sequence boundary, is
414 expressed as a landward thinning wedge of sandy estuarine sediments. Correlation within the
415 Ravenglass estuarine sediment is discussed below and shown in Figures 6, 7, 8 and 9.

416 **7.4 Inner Estuary to River Esk**

417 The Esk channel shows the most complete section of stratigraphy through the cores. The outer
418 estuarine Esk channel correlation is represented by a set of cores along the channel, from core 3 and 1
419 (NE, most upstream) to 7, 8, 10, 12 and 29 (SW, most downstream) (Fig. 6), covering a distance of
420 2.5 km. The channel is composed of a distal meandering river system which becomes wider seaward.
421 All the sediment cores are underlain by the correlatable RGTM which is overlain by fluvial gravel
422 beds, with the exception of cores where the fluvial tidal sands directly overlay the RGTM (e.g., in
423 cores 7 and 8, Fig. 6). The lack of fluvial gravel beds in cores 7 and 8 suggests that the channel
424 thalweg was not present here during the lowstand incision phase. The gravels are thickest in the most
425 upstream, meandering section of the outer estuary (cores 1 and 3) and generally thin downstream
426 (core 10, Fig. 6). The thick fluvial gravel, that accumulated during lowstand in the proximal
427 floodplain, suggests that the River Esk was wider than it is today and appears to show no time lag
428 between progradation of the shelf during lowstand and upstream fluvial aggradation (Cattaneo &
429 Steel, 2003). Fluvial gravel in core 1, drilled in the modern-day floodplain, is 25 cm thick while in
430 core 3, only 185 m away, the fluvial gravel is 3 m thick (Fig. 6). The difference in the thickness of the
431 fluvial gravel from the two cores from the tidal meander (cores 1 and 3; Figs 1 and 6) emphasises the
432 heterogeneity that can occur over short distances.

433 Tidal sand bars, up to 5 m thick, have accumulated in the straighter parts of the Esk channel and have
434 good internal correlation over 500 m (cores 7 and 8, Fig. 6). However, sand bar facies cannot be
435 correlated with cores 1.8 km upstream (cores 1 and 3).

436 Salt and fresh marsh now occurs and can be correlated in all cores in the upper Esk channel (cores 1,
437 3, 7, 8, and 10; Fig. 6) along the channel banks and caps abandoned channels and vegetated bars.

438 **7.5 The River Irt and Central Basin**

439 The River Irt is shown by two northwest – southeast correlation panels, the first highlights cores 22,
440 23, 25, and 26 (Figs. 7 and 8) over 1.45 km. The RGTM is only penetrated in core 25 on panel 1 (Fig.
441 7) and is immediately overlain by a tidal sand bar (cores 25 and 26) (Fig. 1) that fine upwards to mud.
442 The sands show reworked peat clasts implying erosion of pre-existing peat beds nearby. There are
443 thick mud beds at the base of cores 22 and 23 which are overlain by tidal fluvial sands with rare clay
444 drapes and flaser bedding. Tidal sand-, mixed- and mud-flats developed through time indicating the
445 abandonment and reactivation of the River Irt palaeo-channel. The cores of the River Irt and central
446 basin also show no gravel above the limited RGTM indicating that this was possibly a location near
447 the top of the valley walls or interfluves. It is possible that the RGTM and gravels exist deeper in the

448 palaeovalley of the River Irt (Fig. 2) but the boreholes never penetrated the thalweg of the
449 palaeovalley. Lack of peat beds and shell fragments limited the potential for dating of these cores.

450 The second correlation panel of the Irt River arm covers a distance of 0.6 km and (Fig. 8) is shown
451 by cores 18, 19 and 20, located in the active channel, and core 32, located in the floodplain (Fig. 1b).
452 The underlying RGTM and the transgressive peat beds are overlain by tidal fluvial sands. The lack of
453 gravel beds here suggests that the channel thalweg did not incise this location during sea-level fall. As
454 the tidal-fluvial sands were the first estuarine sediment deposits above the peat and till and the
455 coarsest of all sediment in these cores, most likely reflect the migration of the River Irt and ultimately
456 the confluence of all three rivers. The ^{14}C date in the peat in core 18 is $8,094 \pm 32$ yrs BP, which
457 implies the migration occurred after this. However, the subsequent sedimentation in the form of
458 mixed-flats and mud-flats is much younger ($c.634 \pm 26$ yrs BP). The sequence of dates suggests that
459 the recent formation of muddy estuarine deposits ($c.634 \pm 26$ yrs BP) was limited to mud and silt
460 grade material, which is possibly a result of barrier spit formation and dampening of wave action that
461 promoted the recent development of a newly developed central basin at the river confluence. The
462 recent development of tidal flats in the central basin also have been encouraged by the confluence of
463 the three rivers. The correlation panels (Figs. 7 and 8, cores 18, 19, 20, 25, 26) show that, through the
464 past $c.9,000$ yrs BP, the central basin was located on a topographical high, near the valley wall, old
465 palaeo-channels of the floodplain (core 32, 22, 23) are also present. The current channel shows the
466 general sandy thalweg sands and off-channel mixed-flats to mud-flats through the surface deposition
467 (Fig. 8, cores 18, 19, 20).

468 ***7.6 Outer Estuary to Foreshore, Backshore, Tidal Inlet***

469 The foreshore, backshore and tidal inlet are underlain by the RGTM and the gravel beds are limited to
470 core 27 and core 28 (Fig.9). which are interpreted to represent the River Esk palaeo-channel. The
471 gravel beds are thought to be of fluvial origin as they are of a similar thickness to the gravel beds in
472 the inner estuary meandering channel belt (Fig. 6, cores 1 and 3). Fluvial gravel beds are absent in
473 cores 29, 30 and 31 for different reasons. Core 29 shows a sharp transition from the RGTM to peats,
474 indicating that this was a sheltered depression along the Esk valley during sea-level rise. The RGTM
475 in core 31 is immediately overlain by marine sands, potentially implying a major Irt palaeo-channel
476 existed here during the lowstand phase feeding a sand bar in core 31. This interpretation is supported
477 by the mapped palaeo-river Irt in Figure 3. The RGTM was deposited almost 4 m lower in core 31
478 compared to core 30, supporting the interpretation of a palaeo-channel in core 31 and a possible wave
479 ravinement surface in core 30. The limited deposition of sand, and the presence of repeat gravel above
480 the sand in core 30, may imply that this was an area of continued shoreface erosion during shoreline
481 retreat. Wave action may have promoted a landward migration of gravels at this location. The
482 presence of the peat bed and absence of gravels in core 29 above the RGTM (Fig. 9) also reveals that
483 no major channel existed here until the Esk channel migrated as a result of the formation of the barrier

484 spits. Core 30 shows very little in the way of correlation with core 31 over a distance of 0.5 km and
485 their sediment bodies are quite different in both volume and character. The absence of the thicker tidal
486 sand bodies in core 30 suggests that this could have been a wave ravinement surface that
487 progressively moved landward during shoreface retreat. The ravinement surface may have reworked
488 previous deposits and surfaces such as the transgressive systems tract, therefore the wave ravinement
489 surface may also become amalgamated with the sequence boundary. Evidence in the form of
490 reworked peat clasts (Figs. 7, 8 and 9) also suggests extensive reworking of peat beds during this time
491 as channels migrated.

492 ***7.7 Summary of Lateral and Vertical Connectivity***

493 Connectivity within the Ravenglass incised valley sediments is best in the channels that have
494 remained relatively stable during the Holocene transgression. The River Esk panel (Fig. 6) indicates
495 that the initial fluvial-tidal channel sands can be correlated over 2.5 km from the inner to the outer
496 estuary and range in thickness from 1 to 3 m. Tidally influenced sand bars within the channels can be
497 correlated over 0.5 km and range from 3 to 5 m in thickness (Fig. 6, cores 7 and 8), showing similar
498 sediment character but varying thicknesses. 1.8 km upstream of the sand bars, correlation of the
499 fluvial-tidal sands becomes difficult due to the extensive meandering of the tidal channels upstream.
500 The increased heterogeneity upstream is common to all three rivers that feed the system.

501 Peat beds are extensive and thickest in the River Irt floodplain (Fig. 8), ranging from 1.2 m thick in
502 core 32 to 0.2 m downstream in cores 18, 19 and 20 (Fig. 8). Not all the peat beds can be correlated.
503 The tidally-influenced fluvial sands, ranging from 0.8 to 1.5 m in thickness, may be correlated up to
504 1.4 km between cores 22, 23, 25 and 32 (Figs. 7 and 8). The tidally influenced fluvial sands thin
505 towards the active Irt channel to 1.5 m (Figs. 7 and 8) and are not present in cores 18, 19 and 20,
506 located in the active floodplain. A tidally influenced sand bar ranging from 1.6 m to 2.6 m can be
507 correlated ~ 0.2 km along the River Irt (Fig. 7, cores 25 and 26) thinning downstream into tidal flats
508 (Fig. 8, 18, 19, 20). The sand bar is capped with 1.3 m of muds that also thin to 0.5 m downstream
509 towards the channel floodplain (Figs. 7 and 8, cores 22, 23, 18 and 19). The lack of gravels and
510 limited deposition of the RGTM within the cores suggests that the channel thalweg was never
511 penetrated making correlation is more difficult.

512 In the outer estuary, the thickest (6m) tidal fluvial sands are represented by the palaeo-Irt in core 31
513 and show little correlation with core 30, located 0.5 km to the southeast (Fig. 9). The sand bars within
514 the tidal inlet show excellent correlation both laterally and vertically. The tidal sand bars range in
515 thickness from 3.5 to 4.4 m and can be correlated over lengths of ~ 1.5 km.

516 ***8. Synthesis of Valley Creation and Fill***

517 A synthesis of the Ravenglass valley creation, classification and fill throughout the Holocene to
518 present is demonstrated in Figure 10 and is summarised below.

519 According to existing estuary classification schemes (Boyd et al., 2011; Dalrymple et al., 1992; Davis
520 & Dalrymple, 2010), the Ravenglass incised valley-fill is categorised as a small, macro-tidal, mixed
521 wave- to tide-dominated system that initially resulted from coastal plain incision and subsequent
522 transgression. The incision cut through pre-existing glacial stratigraphy (Busby & Merritt, 1999). The
523 creation of the Ravenglass incised valley occurred during the Late Devensian Period (17,000 to
524 12,000 yrs BP), attributed to changes in relative sea-level linked to glacio-isostasy (Figs. 2, 8a). When
525 the maximum period of sea-level fall was reached between c. 12,000-10,500 yrs BP, the present-day
526 coastline was exposed and incised by the Rivers Irt, Esk and Mite (Fig. 8a). According to modelled
527 sea-level curves for the Ravenglass area, the period of incision lasted for 6,500 yrs, between c.18,000-
528 11,500 yrs BP (Lloyd *et al.*, 2013). During this initial phase of valley development, the proto-Drigg
529 and Eskmeal sand spits must have been developing, suggesting a dominant role for wave activity over
530 tidal or fluvial action. Despite the differences in the scale of estuaries, the duration of the Ravenglass
531 incision period is broadly similar to those reported for the Holocene Gironde incised valley, which
532 had an incision period of 8,000 yrs (Allen and Posamentier, 1993) and the Holocene Qiantang River
533 estuary, which had an incision period of ~5,000 yrs BP (Zhang *et al.*, 2014).

534 The presence of basal gravel beds (Figs. 6 and 9) implies that the Early Holocene palaeo-Rivers Esk
535 and Irt had a higher energy than the present-day rivers and a bedload that was capable of cutting
536 through the shelf and forming the Ravenglass valley complex. The post-glacial vegetation may have
537 also favoured rivers carrying gravels and glacial outwash (Kasse *et al.*, 2005). A straighter profile for
538 the palaeo-Rivers Esk, Irt and Mite has been previously proposed by the Halcrow Group (2013). The
539 Irt followed a roughly straight trajectory until at least 410 yrs BP, as evidenced by a historical map by
540 John Speed, published in the year 1610 (Speed, 1610). By 1794, the River Irt had deviated from the
541 SW to NE, following the present-day shoreline and merged with the River Mite (Cary, 1794). At
542 present, there is no published historical map evidence for when the Esk deviated to the north but the
543 absence of fluvial gravels in core 12 (Fig. 6) proves that the deviation happened long after the main
544 Holocene incision phase. The peat bed towards the base of core 12, implies that no fluvial deposition
545 occurred in this sheltered location and that the River Esk did not migrate into the central basin until
546 after the transgressive peat had been deposited.

547 The deeper parts of cores 18, 19, 20 and 32 (Fig. 8) are dominated by peat with negligible sandy
548 sediment. This suggests that the palaeo-River Irt feeding this area, the present-day central basin, had
549 low flow volume and minimal bedload. The absence of fluvial gravel, repetition of peat beds and the
550 young stratigraphic age of the sediment in the central basin ($> 813 \pm 20$ yrs BP, cores 18, 19 and 20)
551 can be used to infer that the River Irt, with its greater flow volume and presumably greater bed load,
552 did not deviate its course to the south and merge with the diminutive River Mite 226 yrs ago.

553 There seems to be no evidence in the map of the depth to glacial till (Fig. 3) for an initial straight path
554 for the Early Holocene paleo-River Esk. The northward migration of the southern Eskmeals spit was
555 probably responsible for the northward deviation of the larger River Esk and its subsequent merger
556 with the smaller River Mite. The capture of the River Esk by the River Mite presumably contributed
557 to the accumulation of the tidal-fluvial sands and the prograding tidal sands and muds in the upper
558 parts of cores 18, 19 and 20 (Fig. 8).

559 **9. Stratigraphic Surfaces of Ravenglass Incised Valley**

560 The stratigraphic organisation and relative stratigraphic surfaces within the Ravenglass incised valley
561 fill are shown in Figure 10 and discussed below.

562 **9.1 Sequence Boundary & Lowstand Systems Tracts - Gravels (LST)**

563 The marine lowstand (12,000 to 10,500 yr BP) of the Late Devensian into the early Holocene (Fig. 2)
564 is categorised as a time when isostatic rebound outstripped sea-level rise (Lloyd et al., 2013; Merritt
565 and Auton, 2000) (Figs. 10, 11a). In the Ravenglass valley, this stratigraphic surface is expressed by
566 the fluvial-alluvial gravels and coarse sands, the base of which marks the sequence boundary with the
567 RGTM. The fluvial gravels and sands have a high preservation potential due to the subsequent rapid
568 onlapping of the transgressive estuarine sediments. During lowstand, sediment was bypassed through
569 the valley and was most likely deposited seaward (west) of the present-day coastline. The rapid
570 lowstand and transgression that the Ravenglass Valley underwent, prior to and into the Holocene,
571 limited the amount of time possible for fluvial aggradation. The gravel beds are thicker in the outer
572 than in the inner estuary (Figs. 6-9) because the palaeo-valleys, on the glacial till surface (Fig. 3),
573 were steeper than the present-day valleys. This resulted in high energy palaeo-rivers capable of
574 carrying gravel further downstream.

575 **9.2 Transgressive Systems Tract - Peat & Estuarine Tidal-Fluvial Sands (TST)**

576 During transgression, after the deposition of the till and gravel, the incised valley was inundated (Figs.
577 10, 11b). This resulted in an accumulation of peat beds in sheltered areas between the main channels,
578 and estuarine tidal-fluvial sands within the tidal channels. The base of the transgressive surface
579 separates the lower fluvial gravels and coarse sands with estuarine peats, sands and muds (Figs. 6-9).
580 In the inner estuarine zone, the surface is well defined particularly along the palaeo-river Esk,
581 however, in contrast, in the River Irt, central basin and outer estuarine zones, the transgressive surface
582 becomes amalgamated with the sequence boundary along the palaeo-valley walls. Contrary to other
583 Holocene estuaries, that typically show large-scale transgressive deposits (Martinsen, 1994; Hori *et*
584 *al.*, 2001; Wilson *et al.*, 2007; Chaumillon *et al.*, 2010b), the Ravenglass estuary demonstrates that
585 most of the backfill began at the end of transgression when maximum accommodation was achieved.
586 Deposition continued into, and throughout, the highstand and falling stage systems tract. The limited
587 accumulation of transgressive deposits within the Ravenglass valley-fill are most likely a result of the

588 rapid transgression and coastal flooding, during which the rate of sea-level rise outpaced sediment
589 supply. The rapid transgression limited the thickness of the aggrading, onlapping sediment within the
590 valley during the landward migration of the coastline, evident in the Esk channel profile (Fig. 6).

591 **9.3 Highstand Systems Tract (HSST) - Tidal Bar Channel Sands, Tidal Meanders,** 592 **Central Basin Muds and Prograding Tidal Sand Bars.**

593 Post-glacial sea-level within the Ravenglass coastal area is estimated to have reached its peak of + 2
594 m OD around 6,000 yrs BP (Lloyd *et al.*, 2013) and has fallen since (Figs. 10, 11c-e). At this peak
595 stage of sea-level rise, accommodation within the valley achieved its maximum point (Figs. 10, 11c-
596 11d). Consequently, infilling of the system mostly occurred during this time, and into, the sea-level
597 regression (Figs. 10, 11d-11e). After 6,000 yrs BP, the falling sea-level formed a seaward-prograding,
598 tide-dominated system consisting of meandering point bars with alternate sand bars, sand-flats, mud-
599 flats, gravels and a small, restricted, muddy central basin with a prograding tidal inlet.

600 Due to the nature of progradation during the highstand-into-regression, the top of the highstand
601 surface is downlapping onto the transgressive estuarine wedge (Figs. 6 and 9). During this time of
602 infilling, the upper estuary tidal limit migrated downstream, promoting fluvial gravel to gradually
603 work its way downstream. This is prominent on the banks of the present day Esk Channel.

604 **9.4 Reservoir Implications**

605 Ravenglass Estuary is a good analogue for assessing simple tide-dominated incised valley-fill models
606 in terms of stratigraphic organisation with the opportunity to analyse a single fill (corresponding to a
607 single sea-level cycle). Although the present day Ravenglass Estuary appears to be mud-rich, the
608 cores (Figs. 6-9) show that majority of the infill is very much sand-dominated. The presence of sand
609 above the sequence boundary implies that, the majority of the coarse-grained sand filling the tidal
610 channels and inlet, is of marine origin. As previously mentioned, this is supported by the presence of
611 shelly detritus hosted in medium to coarse grained sands. Tidal processes have been dominant since
612 the onset of transgression as double clay drapes are recorded in the first sand deposits after the
613 sequence boundary in core 8 (Fig. 6) along the Esk channel. This study is a rare modern analogue of a
614 sandy, tide-dominated estuary. Discussed below is the significance of the Ravenglass sedimentary
615 system for building models of sand/mud ratios, grain size, and sand body connectivity in subsurface
616 reservoirs.

617 **9.4.1 Sand/Mud Ratio & Grain Size**

618 Based on the evidence from 19 Holocene sediment cores, the Ravenglass Estuary-fill is dominated by
619 sand. It should be noted that this interpretation is based on the 19 cores acquired however parts of the
620 subsurface remain unsampled. Although, the localised sand/mud ratio varies from upstream to
621 downstream, sandy deposits typically represent 75% of all cores, the remainder being peat (5%),
622 gravel (10%) and mud (10%) (Figs. 6-9). The upstream meandering portions of the tidal channel

623 system contain greater proportions of interbedded finer grained sand and mud compared to the
624 cleaner, coarser grained sands in the downstream, sinuous portions of the channels (Figs. 5-7). The
625 downstream coarser sands lack well developed mud beds and have accumulated as thick, continuous
626 sands with rare mud drapes (Figs. 6 and 9).

627 The most abundant mud deposition occurred along the River Irt and within the central basin (Figs. 7
628 and 8), which was a result of the backfilling of the River Irt valley and migration to the southeast to
629 merge with the Rivers Mite and Esk. The confluence of all three rivers (Figs 11d-e) allowed for the
630 recent development of the classical tripartite zonation of facies (Boyd et al., 2011; Dalrymple and
631 Zaitlin, 1992); inner estuarine medium-coarse grained sandy tidal channels, mud-rich central basin
632 and marine influenced sands at the estuary mouth.

633 The sand/mud ratio is highest within the marine-influenced tidal inlet and foreshore (Fig. 9). The tidal
634 inlet hosts large incipient tidal bars (Fig. 11e) with limited mud quantities (Fig. 9) due to the
635 remobilisation of bar sediment by the ebb and flood tides. The sand/mud ratio in foreshore sediments
636 is similar to the modern tidal inlet and lacks mud deposition. This lack of mud in the foreshore and
637 tidal inlet can be attributed to the high energy shoreline processes remobilising the sediment and lack
638 of slack water within the tidal inlet.

639 **9.4.2 Connectivity**

640 By analogy to the subsurface, the connectivity of sand is heterogenous across the estuarine system
641 but, as the estuary is sand-dominated, most of the sediment looks as if it has good connectivity. The
642 Esk arm of the estuary represents good reservoir in terms of connectivity (Fig. 5). Tidal fluvial sands
643 and tidally-influenced sand bars (cores 7, 8, 10, 12 and 29) are well connected up to 5.2 km through
644 the river course. The tidal sand bars show varying thickness across the estuary between 4 to 6 m. The
645 Esk system becomes less sandy upstream, promoting reservoir compartmentalisation due to the
646 presence of extensive mud and interfluves (cores 1 and 3). Even under the Saltcoats mudflats, in the
647 River Irt cores 32, 18, 19 and 20 (Figs. 1b, 7) have thin (30-150 cm) correlatable, sand-dominated
648 deposits which become coarser grained towards the thalweg over 1.5 km. The outer Esk, typifying
649 outer estuarine deposits, represents excellent connectivity (cores 27, 28 and 29; Figs. 6 and 9) of
650 sandy sediments ranging from 4 to 6 m . The connectivity of palaeo-Esk and Mite sands is excellent
651 due to the interpretation that the flow path has been stable for about 10,000 yrs (Fig. 11a-e).

652 In contrast to the Esk-Mite system, the palaeo-Irt looks as if it has limited sand connectivity with the
653 palaeo-Esk, as shown by tidal-ravinement deposits in core 30 (Fig. 9) and the palaeotopography map
654 which reveals a high between the River Irt and Esk on the present-day foreshore and in the central
655 basin (Fig. 3). The connectivity of palaeo-Irt and palaeo-Esk-Mite sands is limited due to the recent
656 (between 410-226 yrs BP) merging of the Irt with the Esk-Mite channels (Fig. 11d-e). These

657 observations indicate that channel migration can happen in a short time period (~10 ka), resulting in
658 complicated reservoir architecture.

659 **10. Synthesis**

660 This study of the Ravenglass incised valley, post-glacial fill provides a practical means of
661 highlighting the facies distributions and stratigraphic differences of glacio-induced estuaries of
662 macro-tidal, tide-dominated settings. This paper has revealed the characteristics of the estuary that
663 have developed in the palaeo-Ravenglass incised valley during the last transgression. This has been
664 achieved using 19 cores drilled into the Holocene estuarine sediment, and sediment facies analysis,
665 sediment distribution and high-resolution ^{14}C ages.

666 We propose that Ravenglass valley formed and subsequently filled in five identifiable stages:

667 1. The Devensian glacial lowstand, when isostatic rebound outstripped sea-level rise, between 12,000-
668 10,500 yrs BP (Fig. 2). This promoted shelf incision represented by the fluvial-alluvial gravel
669 overlying the Ravenglass Glacial Till Member (Figs. 10, 11a). Fluvial processes were dominant and
670 net sediment was bypassed to the lowstand shelf. During this time there was a basinward shift in
671 facies (Figs. .

672 2. The Early Holocene rapid transgression, which was characterised by a phase of relative sea-level
673 rise, occurring between c.10,500-6,000 yrs BP (Fig. 2). During this time, net sediment transport was
674 landward with transgressive sediments onlapping alluvial gravels or the Ravenglass Glacial Till
675 Member where the gravels were not present (Fig 10, 11b). This resulted in estuarine deposition, with
676 peats initially forming on locally isolated highs, between channels, and the transitional fluvial-
677 estuarine sands subsequently filling the deepest part of the valleys. During this time, it is here
678 suggested that much of the sand supplied to the estuary was of marine origin due to the presence of
679 shelly debris. Sea-level rapidly outpaced sediment supply, limiting the amount of time for the
680 transgressive estuarine deposits to form. The transgressive deposits are therefore relatively thin. As
681 the first transgressive deposits are sandy, it implies a reasonable amount of sand was available on the
682 shelf to be reworked into the valley by tidal currents.

683 3. The Holocene highstand, which occurred as sea-level stabilised, and accommodation reached its
684 maximum point at around 6,000 to 5,000 yrs BP (Figs. 10, 11c). Back-filling of the Irt and Esk
685 valleys continued at this time. The stabilising of sea-level and dominant wave-action may have
686 promoted the growth of the palaeo-Drigg and Eskmeals Spits. Despite increased wave action, tidal
687 signatures were still prevalent in the estuarine sediment since the onset of deposition. The spits
688 demonstrate that wave-dominated elements can play an important role in the evolution of tide-
689 dominated systems.

690 4. A minor fall in relative sea level from 5,000 yrs BP to the present day, resulting in the estuarine
691 system filling and prograding (Figs. 10, 11d). In-channel tidal bars started to build in the downstream
692 tidal channels, upstream meanders prograded and the system stepped seaward. Radiocarbon dating
693 suggests that most of the fill occurred during the highstand to falling stage systems tract, highlighting
694 that not all estuarine sedimentation corresponds to the transgressive phase.

695 5. Complete backfill of the Irt and Esk channels is the final stage (~ 410 to 226 yrs BP, Fig. 11e). This
696 was possibly coincident with the southward migration of the Drigg spit which closed off the mouth
697 River Irt which thus forced the merging of the Irt with the Rivers Mite and Esk to adopt the present-
698 day morphology.

699 These stages of evolution within the Ravenglass incised valley system have resulted in a particular
700 facies organisation not widely discussed in the literature. The stratigraphic relationships and facies
701 models (Figs. 6-9) enable the construction of a detailed depositional model of the Ravenglass incised
702 valley-fill.

703 The results of this study can be used to interpret the development of several other, mixed energy
704 macrotidal estuaries in the stratigraphic rock record, that may also correspond to late transgressive –
705 highstand conditions. It may also be used to predict reservoir architecture, lateral and vertical
706 connectivity and sand quality within such a system.

707 The work presented here can be used to predict connectivity and sand-quality within incised valley-
708 fill sediments. The Esk-Mite system has very good connectivity and sand quality, largely due to the
709 stability of the flow path of the rivers. The Irt, in contrast, is poorly connected to the Esk-Mite system
710 because of the relatively recent southward deflection of the flow path and consequent merging of the
711 rivers. Sand-mud ratios decrease upstream in both the Irt and Esk estuarine fills. The coarsest and
712 cleanest sands are found in the tidal inlet and on the foreshore.

713 **Acknowledgments**

714 This work was undertaken as a joint project between Newcastle University and The University of
715 Liverpool's Chlorite Consortium. We thank editors Victoria Valdez and Ian Kane and also reviewers
716 Martin Wells and Benjamin Brigaud for their very helpful comments in refining this manuscript.

717

718

719 **References**

720 **Ainsworth, R.B., Vakarelov, B.K. and Nanson, R.A.** (2011) Dynamic spatial and temporal
721 prediction of changes in depositional processes on clastic shorelines: Toward improved
722 subsurface uncertainty reduction and management. *AAPG Bulletin*, **95**, 267–297.

- 723 **Allen, G.P. and H. W. Posamentier** (1993) Sequence Stratigraphy and Facies Model of an Incised
724 Valley Fill: The Gironde Estuary, France. *SEPM Journal of Sedimentary Research*, **Vol. 63**,
725 378–391.
- 726 **Assinder, D.J., Kelly, M. and Aston, S.R.** (1985) Tidal variations in dissolved and particulate phase
727 radionuclide activities in the Esk estuary, England, and their distribution coefficients and
728 particulate activity fractions. *Journal of Environmental Radioactivity*, **2**, 1–22.
- 729 **Bonsall, C., Sutherland, D., Tipping, R. and Cherry, J.** (1989) The Eskmeals Project: late
730 Mesolithic settlement and environment in north-west England. *The Mesolithic in Europe*, 175–
731 205.
- 732 **Bousher, A.** (1999) Ravenglass Estuary: Basic characteristics and evaluation of restoration options.
733 *RESTRAT Technical Deliverable TD*, 12.
- 734 **Boyd Ron, Robert W. Dalrymple, K.C. and Zaitlin, B.A.** (2011) Estuarine and Incised-Valley
735 Facies Models. 171–235 pp.
- 736 **Busby, J.P. and Merritt, J.W.** (1999) Quaternary deformation mapping with ground penetrating
737 radar. *Journal of Applied Geophysics*, **41**, 75–91.
- 738 **Cattaneo, A. and Steel, R.J.** (2003) Transgressive deposits: A review of their variability. *Earth-*
739 *Science Reviews*, **62**, 187–228.
- 740 **Chaumillon, E., Tessier, B. and Reynaud, J.-Y.** (2010a) Stratigraphic records and variability of
741 incised valleys and estuaries along French coasts. *Bulletin de la Société Géologique de France*,
742 **181**, 75–85.
- 743 **Chaumillon, E., Tessier, B. and Reynaud, J.Y.** (2010b) Stratigraphic records and variability of
744 Incised valleys and estuaries along French coasts. *Bulletin de la Societe Geologique de France*,
745 **181**, 75–85.
- 746 **Clare, T., Clapham, A.J., Wilkinson, D.M. and Haworth, E.Y.** (2001) The Mesolithic and
747 Neolithic landscapes of Barfield Tarn and Eskmeals in the English Lake District: some new
748 evidence from two different wetland contexts. *Journal of Wetland Archaeology*, **1**, 83–105.
- 749 **Coast, D. and Area, S.** (2015) Drigg Coast SAC , Ravenglass Estuary Intertidal Survey.
- 750 **Dalrymple, R.W., Canada, O.K.L. and Zaitlin, B.A.** (1992a) Estuarine Facies Models: Conceptual
751 Basis and Stratigraphic Implications: PERSPECTIVE. *Journal of Sedimentary Petrology*, **62**,
752 1130–1146.
- 753 **Dalrymple, R.W. and Zaitlin, B.A.** (1994) High-resolution sequence stratigraphy of a complex,
754 incised valley succession, Cobequid Bay — Salmon River estuary, Bay of Fundy, Canada.
755 *Sedimentology*, **41**, 1069–1091.
- 756 **Dalrymple, R.W., Zaitlin, B.A. and Boyd, R.** (1992b) Estuarine facies models; conceptual basis and
757 stratigraphic implications. *Journal of Sedimentary Research*, **62**, 1130–1146.
- 758 **Davis, R.A. and Dalrymple, R.W.** (2010) Principles of tidal sedimentology. 1–621 pp.
- 759 **Delaney, C.** (2003) The last glacial stage (the Devensian) in northwest England. *North West*
760 *geography*, **3**, 27–37.
- 761 **Fenies, H. and Tastet, J.P.** (1998) Facies and architecture of an estuarine tidal bar (the Trompeloup
762 bar, Gironde Estuary, SW France). *Marine Geology*, **150**, 149–169.
- 763 **Garrison, J.R. and Bergh, T.C.V. Van Den** (2006) Effects of sedimentation rate, rate of relative rise
764 in sea level, and duration of sea-level cycle on the filling of incised valleys: examples of filled
765 and “overfilled” incised valleys from the upper Ferron Sandstone, Last Chance Delta, east-
766 central Utah. 239–279 pp.

- 767 **Geyer, W.R.** (1993) The importance of suppression of turbulence by stratification on the estuarine
768 turbidity maximum. *Estuaries*, **16**, 113–125.
- 769 **Griffiths, J., Worden, R.H., Wooldridge, L.J., Utley, J.E.P. and Duller, R.A.** (2018) Detrital Clay
770 Coats, Clay Minerals, and Pyrite: A Modern Shallow-Core Analogue For Ancient and Deeply
771 Buried Estuarine Sandstones. *Journal of Sedimentary Research*, **88**, 1205–1237.
- 772 **Griffiths, J., Worden, R.H., Wooldridge, L.J., Utley, J.E.P., Duller, R.A. and Edge, R.L.** (2019)
773 Estuarine clay mineral distribution: Modern analogue for ancient sandstone reservoir quality
774 prediction. *Sedimentology*, **66**, 2011–2047.
- 775 **Halcrow Group** (2013) Ravenglass Estuary Complex Sefton Council.
- 776 **Hampson, G.J., Da Vies, S.J., Elliott, T., Flint, S.S. and Stollhofen, H.** (1999) Incised valley fill
777 sandstone bodies in Upper Carboniferous fluvio-deltaic strata: Recognition and reservoir
778 characterization of Southern North Sea analogues. *Petroleum Geology Conference Proceedings*,
779 **5**, 771–788.
- 780 **Heap, A.D., Bryce, S. and Ryan, D.A.** (2004) Facies evolution of Holocene estuaries and deltas: A
781 large-sample statistical study from Australia. *Sedimentary Geology*, **168**, 1–17.
- 782 **Hein, F.J.** (2015) The Cretaceous McMurray oil sands, Alberta, Canada: A world-class, tidally
783 influenced fluvial-estuarine system-An Alberta government perspective, 1st edn. *Elsevier B.V.*,
784 561–562 pp.
- 785 **Hori, K., Saito, Y., Zhao, Q., Cheng, X., Wang, P., Sato, Y. and Li, C.** (2001) Sedimentary facies
786 of the tide-dominated paleo-Changjiang (Yangtze) estuary during the last transgression. *Marine*
787 *Geology*, **177**, 331–351.
- 788 **Jalón-Rojas, I., Schmidt, S. and Sottolichio, A.** (2015) Turbidity in the fluvial Gironde Estuary
789 (southwest France) based on 10-year continuous monitoring: Sensitivity to hydrological
790 conditions. *Hydrology and Earth System Sciences*, **19**, 2805–2819.
- 791 **Kasse, C., Hoek, W.Z., Bohncke, S.J.P., Konert, M., Weijers, J.W.H., Cassee, M.L. and van der**
792 **Zee, R.M.** (2005) Late Glacial fluvial response of the Niers-Rhine (western Germany) to
793 climate and vegetation change. *Journal of Quaternary Science*, **20**, 377–394.
- 794 **Kelly, M., Emptage, M., Mudge, S., Bradshaw, K. and Hamilton-Taylor, J.** (1991) The
795 relationship between sediment and plutonium budgets in a small macrotidal estuary: Esk estuary,
796 Cumbria, UK. *Journal of Environmental Radioactivity*, **13**, 55–74.
- 797 **Kershaw, P.J., Woodhead, D.S., Malcolm, S.J., Allington, D.J. and Lovett, M.B.** (1990) A
798 Sediment History of Sellafield Discharges. *Journal of Environmental Radioactivity*, **12**, 201–
799 241.
- 800 **Lloyd, J.M., Zong, Y., Fish, P. and Innes, J.B.** (2013) Holocene and Lateglacial relative sea-level
801 change in north-west England: Implications for glacial isostatic adjustment models. *Journal of*
802 *Quaternary Science*, **28**, 59–70.
- 803 **Martinsen, O.J.** (1994) Evolution of an incised-valley fill, the Pine Ridge Sandstone of southeastern
804 Wyoming, USA: systematic sedimentary response to relative sea-level change. *Incised Valley*
805 *Systems: Origin and Sedimentary Sequences*, *SEPM Special Publication*, 109–128.
- 806 **Meng, J., Holubnyak, Y., Hasiuk, F., Hollenbach, J. and Wreath, D.** (2020) Geological
807 characterization of the Patterson CO₂ storage site from 3-D seismic data. *Midcontinent*
808 *Geoscience*, **1**, 52–90.
- 809 **Menier, D., Tessier, B., Proust, J.N., Baltzer, A., Sorrel, P. and Traini, C.** (2010) The Holocene
810 transgression as recorded by incised-valley infilling in a rocky coast context with low sediment
811 supply (southern Brittany, western France). *Bulletin de la Societe Geologique de France*, **181**,

- 812 115–128.
- 813 **Merritt, J.W. and Auton, C.A.** (2000) An outline of the lithostratigraphy and depositional history of
814 Quaternary deposits in the Sellafield district, west Cumbria. *Proceedings of the Yorkshire*
815 *Geological Society*, **53**, 129–154.
- 816 **Royd, D.O.** (2002) Chapter 19: The glaciation of the Lake District. *Geological Society Memoir*, **25**,
817 255–269.
- 818 **Salem, A.M., Ketzer, J.M., Morad, S., Rizk, R.R. and Al-Aasm, I.S.** (2005) Diagenesis and
819 Reservoir-Quality Evolution of Incised-Valley Sandstones: Evidence from the Abu Madi Gas
820 Reservoirs (Upper Miocene), the Nile Delta Basin, Egypt. *Journal of Sedimentary Research*, **75**,
821 572–584.
- 822 **Sanford, L.P., Suttles, S.E. and Halka, J.P.** (2001) Reconsidering the physics of the Chesapeake
823 Bay estuarine turbidity maximum. *Estuaries*, **24**, 655–669.
- 824 **Simon, N., Worden, R.H., Muhammed, D.D., Utley, J.E.P., Verhagen, I.T.E., Griffiths, J. and**
825 **Wooldridge, L.J.** (2021) Sediment textural characteristics of the Ravenglass Estuary;
826 Development of a method to predict palaeo sub-depositional environments from estuary core
827 samples. *Sedimentary Geology*, **418**, 105906.
- 828 **Slatt, R.M.** (2013) Fluvial deposits and reservoirs. 283–369 pp.
- 829 **Tessier, B.** (2012) Stratigraphy of Tide-Dominated Estuaries. In: *Principles of Tidal Sedimentology*,
830 2012, 109–128.
- 831 **Virolle, M., Brigaud, B., Luby, S., Portier, E., Féliès, H., Bourillot, R., Patrier, P. and Beaufort,**
832 **D.** (2019) Influence of sedimentation and detrital clay grain coats on chloritized sandstone
833 reservoir qualities: Insights from comparisons between ancient tidal heterolithic sandstones and
834 a modern estuarine system. *Marine and Petroleum Geology*, **107**, 163–184.
- 835 **Virolle, M., Féliès, H., Brigaud, B., Bourillot, R., Portier, E., Patrier, P., Beaufort, D., Jalon-**
836 **Rojas, I., Derriennic, H. and Miska, S.** (2020) Facies associations, detrital clay grain coats and
837 mineralogical characterization of the Gironde estuary tidal bars: A modern analogue for deeply
838 buried estuarine sandstone reservoirs. *Marine and Petroleum Geology*, **114**, 104225.
- 839 **Wang, R., Colombera, L. and Mountney, N.P.** (2019) Geological controls on the geometry of
840 incised-valley fills: Insights from a global dataset of late-Quaternary examples. *Sedimentology*,
841 **66**, 2134–2168.
- 842 **Wang, R., Colombera, L. and Mountney, N.P.** (2020) Quantitative analysis of the stratigraphic
843 architecture of incised-valley fills: A global comparison of Quaternary systems. *Earth-Science*
844 *Reviews*, **200**, 102988.
- 845 **Wells, J.T.** (1995) Chapter 6 Tide-dominated estuaries and tidal rivers. *Developments in*
846 *Sedimentology*, **53**, 179–205.
- 847 **Willis, B.J. and Gabel, S.** (2001) Sharp-based, tide-dominated deltas of the {Sego} {Sandstone},
848 {Book} {Cliffs}, {Utah}, {USA}. *Sedimentology*, **48**, 479–506.
- 849 **Wilson, K., Berryman, K., Cochran, U. and Little, T.** (2007) A Holocene incised valley infill
850 sequence developed on a tectonically active coast: Pakarae River, New Zealand. *Sedimentary*
851 *Geology*, **197**, 333–354.
- 852 **Wooldridge, L.J., Worden, R.H., Griffiths, J., Thompson, A. and Chung, P.** (2017a) Biofilm
853 origin of clay-coated sand grains. *Geology*, **45**, 875–878.
- 854 **Wooldridge, L.J., Worden, R.H., Griffiths, J. and Utley, J.E.P.** (2019) Clay-coat diversity in
855 marginal marine sediments. *Sedimentology*, **66**, 1118–1138.

- 856 **Wooldridge, L.J., Worden, R.H., Griffiths, J. and Utley, J.E.P.** (2017b) Clay-Coated Sand Grains
857 In Petroleum Reservoirs: Understanding Their Distribution Via A Modern Analogue. *Journal of*
858 *Sedimentary Research*, **87**, 338–352.
- 859 **Wooldridge, L.J., Worden, R.H., Griffiths, J., Utley, J.E.P. and Thompson, A.** (2018) The origin
860 of clay-coated sand grains and sediment heterogeneity in tidal flats. *Sedimentary Geology*, **373**,
861 191–209.
- 862 **Zaitlin, B.A., Dalrymple, R.W. and Boyd, R.** (1994) The Stratigraphic Organization of Incised-
863 Valley Systems Associated with Relative Sea-Level Change. *Incised-Valley Systems: Origin*
864 *and Sedimentary Sequences* 51:0.
- 865 **Zhang, X., Lin, C.M., Dalrymple, R.W., Gao, S. and Li, Y.L.** (2014) Facies architecture and
866 depositional model of a macrotidal incised-valley succession (Qiantang River estuary, eastern
867 China), and differences from other macrotidal systems. *Bulletin of the Geological Society of*
868 *America*, **126**, 499–522.
- 869 **Zong, Y. and Tooley, M.J.** (1996) Holocene sea-level changes and crustal movements in Morecambe
870 Bay, northwest England. *Journal of Quaternary Science*, **11**, 43–58.
- 871